

**STREAMFLOW EXTREMES AND CLIMATE VARIABILITY IN  
SOUTHEASTERN UNITED STATES**

by

Jenna Bobsein

A Thesis Submitted to the Faculty of  
the College of Engineering and Computer Science  
in Partial Fulfillment of the Requirements for the Degree of  
Master of Science

Florida Atlantic University

Boca Raton, Florida

May 2015

Copyright © 2015 by Jenna Bobsein

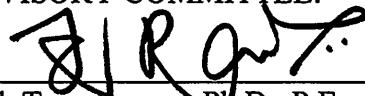
**STREAMFLOW EXTREMES AND CLIMATE VARIABILITY IN  
SOUTHEASTERN UNITED STATES**

by

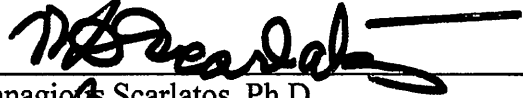
Jenna Bobsein

This thesis was prepared under the direction of the candidate's thesis advisor, Dr. Ramesh Teegavarapu, Department of Civil, Environmental, and Geomatics Engineering, and has been approved by the members of her supervisory committee. It was submitted to the faculty of the College of Engineering and Computer Science and was accepted in partial fulfillment of the requirements for the degree of Master of Science.

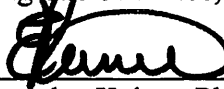
SUPERVISORY COMMITTEE:



Ramesh Teegavarapu, Ph.D., P.E.  
Thesis Advisor



Panagiotis Scarlatos, Ph.D.



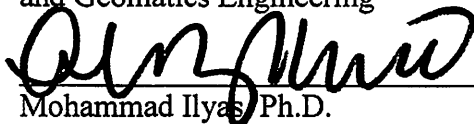
Evangelos Kaisar, Ph.D.



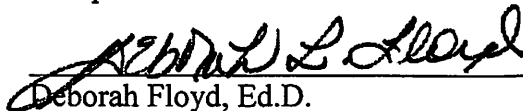
Sudhagar Nagarajan, Ph.D.



Yan Yong, Ph.D.  
Chair, Department of Civil, Environmental  
and Geomatics Engineering



Mohammad Ilyas, Ph.D.  
Dean, College of Engineering and  
Computer Science



Deborah Floyd, Ed.D.  
Dean, Graduate College

4/7/15

Date

## **ABSTRACT**

Author: Jenna Bobsein

Title: Streamflow Extremes and Climate Variability in Southeastern United States

Institution: Florida Atlantic University

Thesis Advisor: Dr. Ramesh Teegavarapu

Degree: Master of Science

Year: 2015

Trends in streamflow extremes at a regional scale linked to the possible influences of four major oceanic-atmospheric oscillations are analyzed in this study. Oscillations considered include: El Niño Southern Oscillation (ENSO), Pacific Decadal Oscillation (PDO), Atlantic Multidecadal Oscillation (AMO), and North Atlantic Oscillation (NAO). The main emphasis is low flows in the South-Atlantic Gulf region of the United States. Several standard drought indices of low flow extremes during two different phases (warm/positive and cool/negative) of these oscillations are evaluated. Long-term streamflow data at 43 USGS sites in the region from the Hydro-Climatic Data Network that are least affected by anthropogenic influences are used for analysis. Results show that for ENSO, low flow indices were more likely to occur during La Niña phase; however, longer deficits were more likely during El Niño phase. Results also show that for PDO (AMO), all (most) low flow indices occur during the cool (warm) phase.

## **ACKNOWLEDGEMENTS**

I would like to sincerely thank my advisor, Dr. Ramesh Teegavarapu, for all of his guidance and support during the writing of this manuscript. Working with Dr. T has been an extremely rewarding experience and I am very grateful for everything I have learned from him.

**STREAMFLOW EXTREMES AND CLIMATE VARIABILITY IN  
SOUTHEASTERN UNITED STATES**

LIST OF TABLES .....	x
LIST OF FIGURES .....	xii
LIST OF ACRONYMS .....	xv
1 INTRODUCTION .....	1
1.1 Background .....	1
1.2 Study Domain.....	1
1.3 Climate Oscillations and Streamflow Extremes.....	3
1.3.1 Climate Oscillations.....	3
1.3.2 Streamflow Extremes.....	3
1.3.3 Oceanic-Atmospheric Influences on Streamflows.....	4
1.4 Problem Statement .....	4
1.5 Objectives of the Study .....	5
1.6 Thesis Organization.....	6
2 LITERATURE REVIEW .....	7
2.1 Oceanic-Atmospheric Variability .....	7
2.1.1 El Niño-Southern Oscillation (ENSO).....	7

2.1.2	Pacific Decadal Oscillation (PDO) .....	8
2.1.3	Atlantic Multidecadal Oscillation (AMO) .....	10
2.1.4	North Atlantic Oscillation (NAO) .....	11
2.2	Methods of Analysis.....	12
2.2.1	Precipitation Extremes and Variations.....	12
2.2.2	Streamflow Variations .....	13
3	METHODS OF ANALYSIS .....	17
3.1	Flow Duration Curves .....	18
3.2	Low Flow Frequency Analysis .....	19
3.2.1	Estimates of 7Q10 Low Flow Index .....	19
3.2.2	7Q10 Statistical Significance Analysis.....	21
3.2.3	Temporal Variability Analysis.....	22
3.3	Streamflow Deficit.....	23
4	STUDY DOMAIN.....	26
4.1	Study Region.....	26
4.2	Data Sets.....	27
4.1.1	Streamflow Data .....	27
4.1.2	Warm and Cool Phases of Oscillations.....	33
5	RESULTS AND ANALYSIS.....	36
5.1	Flow Duration Curves .....	37

5.1.1	El Niño – Southern Oscillation .....	37
5.1.2	Pacific Decadal Oscillation.....	42
5.1.3	Atlantic Multidecadal Oscillation.....	45
5.1.4	North Atlantic Oscillation.....	48
5.2	Low Flow Frequency Analysis .....	53
5.2.1	El Niño – Southern Oscillation.....	53
5.2.2	Pacific Decadal Oscillation.....	55
5.2.3	Atlantic Multidecadal Oscillation.....	57
5.2.4	North Atlantic Oscillation.....	60
5.3	7Q10 Statistical Significance Analysis .....	63
5.4	Temporal Variability Analysis.....	63
5.4.1	El Niño-Southern Oscillation.....	64
5.4.2	Pacific Decadal Oscillation.....	66
5.4.3	Atlantic Multidecadal Oscillation.....	68
5.4.4	North Atlantic Oscillation.....	70
5.5	Streamflow Deficit .....	71
5.5.1	El Niño-Southern Oscillation.....	71
5.5.2	Pacific Decadal Oscillation.....	74
5.5.3	Atlantic Multidecadal Oscillation.....	77
5.5.4	North Atlantic Oscillation.....	82



5.6	Influences of AMO Phases on Spatial Variability of Streamflow Extremes in Florida.....	85
5.6.1	Florida Southern Peninsular Region .....	86
5.6.2	Florida Northern Continental Region .....	89
6	CONCLUSIONS.....	93
6.1	Contributions of this Study .....	93
6.1.1	El Niño – Southern Oscillation.....	94
6.1.2	Pacific Decadal Oscillation.....	95
6.1.3	Atlantic Multidecadal Oscillation.....	95
6.1.4	North Atlantic Oscillation.....	96
6.2	Limitations of this Study .....	97
6.3	Recommendations for Future Research .....	97
	REFERENCES .....	99

## LIST OF TABLES

Table 1: Case Study Streamflow Data Station List (Part 1) .....	30
Table 2: Case Study Streamflow Data Station List (Part 2) .....	31
Table 3: Temporal Windows for El Niño and La Niña Phases of ENSO.....	34
Table 4: Temporal Windows for Warm and Cool Phases of PDO .....	34
Table 5: Temporal Windows for Warm and Cool Phases of AMO.....	34
Table 6: Temporal Windows for Positive and Negative Phases of NAO.....	35
Table 7: FDC-based Low Flow Occurrences for ENSO El Niño and La Niña Phases ....	38
Table 8: FDC-based Low Flow Occurrences for ENSO El Niño and La Niña Phases (Group 1).....	40
Table 9: FDC-based Low Flow Occurrences for ENSO El Niño and La Niña Phases (Group 2).....	40
Table 10: FDC-based Low Flow Occurrences for PDO Warm and Cool Phases .....	43
Table 11: FDC-based Low Flow Occurrences for AMO Warm and Cool Phases .....	46
Table 12: FDC-based Low Flow Occurrences for NAO Positive and Negative Phases ..	49
Table 13: FDC-based Low Flow Occurrences for NAO Positive and Negative Phases (Group 1).....	51
Table 14: FDC-based Low Flow Occurrences for NAO Positive and Negative Phases (Group 2).....	51
Table 15: 7Q10 Values for ENSO El Niño and La Niña Phases .....	54
Table 16: 7Q10 Values for PDO Warm and Cool Phases .....	56

Table 17: 7Q10 Values for AMO Warm and Cool Phases .....	58
Table 18: 7Q10 Values for NAO Positive and Negative Phases .....	60
Table 19: 7Q10 Values for NAO Positive and Negative Phases (Group 1) .....	62
Table 20: 7Q10 Values for NAO Positive and Negative Phases (Group 2) .....	62
Table 21: Streamflow Deficit Duration Analysis for El Niño and La Niña Phases of ENSO .....	72
Table 22: Streamflow Deficit Duration Analysis for Warm and Cool Phases of PDO ....	75
Table 23: Streamflow Deficit Duration Analysis for Warm and Cool Phases of AMO... 78	
Table 24: Streamflow Deficit Duration Analysis for Warm and Cool Phases of AMO (Group 1).....	80
Table 25: Streamflow Deficit Duration Analysis for Warm and Cool Phases of AMO (Group 2).....	80
Table 26: Streamflow Deficit Duration Analysis for Positive and Negative Phases of NAO.....	83
Table 27: 7Q10 Values for AMO Warm and Cool Phases (Florida Southern Peninsula Region).....	88
Table 28: 7Q10 Values for AMO Warm and Cool Phases (Florida Northern Continental Region).....	91

## LIST OF FIGURES

Figure 1: USGS HUC Regions in the U.S. (Seaber <i>et al.</i> , 1987).....	2
Figure 2: Anomalous Climate Conditions Associated with Warm Phase PDO (Mantua and Hare, 2002) .....	9
Figure 3: Spatial Coverage of AMO Influence (Pierce, 2013) .....	10
Figure 4: NAO Index 1864 – 1995 (Hurrell and Van Loon, 1997) .....	11
Figure 5: Methodology for Evaluation of Trends in Streamflow Extremes and Climate Variability.....	17
Figure 6: Definition of Deficit Characteristics (Hisdal, 2008) .....	24
Figure 7: Climate Regions within HUC Region 03 Based on the Köppen-Geiger Climate Classification (Kottek <i>et al.</i> , 2006) .....	27
Figure 8: HCDN Stations Used for this Study .....	32
Figure 9: HCDN Stations used for this Study Divided by Geographic Location.....	33
Figure 10: Variability of FDC due to ENSO .....	39
Figure 11: FDCs of El Niño and La Niña Phases of ENSO at Select Stations (Group 1) .....	41
Figure 12: FDCs of El Niño and La Niña Phases of ENSO at Select Stations (Group 2) .....	42
Figure 13: Variability of FDC due to PDO.....	44
Figure 14: FDCs of Warm and Cool Phases of PDO at Select Stations (Group 1) .....	45
Figure 15: FDCs of Warm and Cool Phases of PDO at Select Stations (Group 2) .....	45

Figure 16: Variability of FDC due to AMO .....	47
Figure 17: FDCs of Warm and Cool Phases of AMO at Select Stations (Group 1).....	48
Figure 18: FDCs of Warm and Cool Phases of AMO at Select Stations (Group 2).....	48
Figure 19: Variability of FDC due to NAO .....	50
Figure 20: FDCs of Positive and Negative Phases of NAO at Select Stations (Group 1)	52
Figure 21: FDCs of Positive and Negative Phases of NAO at Select Stations (Group 2)	53
Figure 22: Variability of 7Q10 due to ENSO .....	55
Figure 23: Variability of 7Q10 due to PDO.....	57
Figure 24: Variability of 7Q10 due to AMO .....	59
Figure 25: Variability of 7Q10 due to NAO.....	61
Figure 26: Kernel Density Estimates of AM7 Occurrences for El Niño and La Niña Phases of ENSO (a) All Stations, (b) Group 1, (c) Group 2 .....	64
Figure 27: Kernel Density Estimates of AM7 Occurrences for Warm and Cool Phases of PDO (a) All Stations, (b) Group 1, (c) Group 2.....	66
Figure 28: Kernel Density Estimates of AM7 Occurrences for Warm and Cool Phases of AMO (a) All Stations, (b) Group 1, (c) Group 2.....	68
Figure 29: Kernel Density Estimates of AM7 Occurrences for Positive and Negative Phases of NAO (a) All Stations, (b) Group 1, (c) Group 2 .....	70
Figure 30: Variability of Deficit Durations due to ENSO .....	73
Figure 31: Cumulative Probability Plots of Streamflow Deficit Duration for El Niño and La Niña Phases of ENSO at Select Stations (Group 1).....	74
Figure 32: Cumulative Probability Plots of Streamflow Deficit Duration for El Niño and La Niña Phases of ENSO at Select Stations (Group 2).....	74

Figure 33: Variability of Deficit Durations due to PDO.....	76
Figure 34: Cumulative Probability Plots of Streamflow Deficit Duration for Warm and Cool Phases of PDO at Select Stations (Group 1).....	77
Figure 35: Cumulative Probability Plots of Streamflow Deficit Duration for Warm and Cool Phases of PDO at Select Stations (Group 2).....	77
Figure 36: Variability of Deficit Durations due to AMO .....	79
Figure 37: Cumulative Probability Plots of Streamflow Deficit Duration for Warm and Cool Phases of AMO at Select Stations (Group 1) .....	81
Figure 38: Cumulative Probability Plots of Streamflow Deficit Duration for Warm and Cool Phases of AMO at Select Stations (Group 2) .....	82
Figure 39: Variability of Deficit Durations due to NAO .....	84
Figure 40: Cumulative Probability Plots of Streamflow Deficit Duration for Positive and Negative Phases of NAO at Select Stations (Group 1) .....	85
Figure 41: Cumulative Probability Plots of Streamflow Deficit Duration for Positive and Negative Phases of NAO at Select Stations (Group 2) .....	85
Figure 42: FDCs of Warm and Cool Phases of AMO (Florida Southern Peninsular Region) .....	87
Figure 43: Cumulative Probability Plots of Streamflow Deficit Duration for Warm and Cool Phases of AMO (Florida Southern Peninsular Region).....	88
Figure 44: FDCs of Warm and Cool Phases of AMO (Florida Northern Continental Region) .....	90
Figure 45: Cumulative Probability Plots of Streamflow Deficit Duration for Warm and Cool Phases of AMO (Florida Northern Continental Region).....	92

## LIST OF ACRONYMS

AM7	7-day average minimum value
AMO	Atlantic Multidecadal Oscillation
DD	Deficit Duration
ENSO	El Niño-Southern Oscillation
EP	Exceedance Probability
FDC	Flow Duration Curve
HCDN	Hydro-Climatic Data Network
HUC	Hydrologic Unit Code
KDE	Kernel Density Estimate
KS	Kolmogorov-Smirnov
MLE	Maximum Likelihood Estimation
NAO	North Atlantic Oscillation
NEP	Non-exceedance Probability
PDO	Pacific Decadal Oscillation
PNA	Pacific-North American teleconnection pattern
SST	Sea Surface Temperature
USGS	United States Geological Survey

# 1 INTRODUCTION

## 1.1 Background

According to the U.S. Geological Survey (USGS), of all the potential threats posed by climatic variability and change, those associated with water resources are the most consequential for both society and the environment (Lins *et al.*, 2010). In addition to increases in global average air and ocean temperatures, observations find increasing occurrences of extreme weather, including low flows and droughts (USGS, 2007). Understanding changes in the distribution, quantity and quality of, and demand for water in response to climate variability and change is essential to planning for and adapting to future climatic conditions (Lins *et al.*, 2010).

## 1.2 Study Domain

The scope of this project will focus solely on streamflows in the southeastern United States, specifically in USGS hydrologic unit code (HUC) region 03. The United States is divided and subdivided into successively smaller hydrologic units which are classified into four levels: regions, sub-regions, according units, and cataloging units (Seaber *et al.*, 1987). The hydrologic units are nested within each other, from the largest geographic area (regions) to the smallest (cataloging units). The first level of classification divides the United States into 21 major regions based on surface topography. These regions contain either the drainage area of a major river (such as the Missouri region) or the



combined drainage area of a series of rivers (such as the Texas-Gulf region) (Seaber *et al.*, 1987). The 21 major HUC regions of the United States are shown in Figure 1.

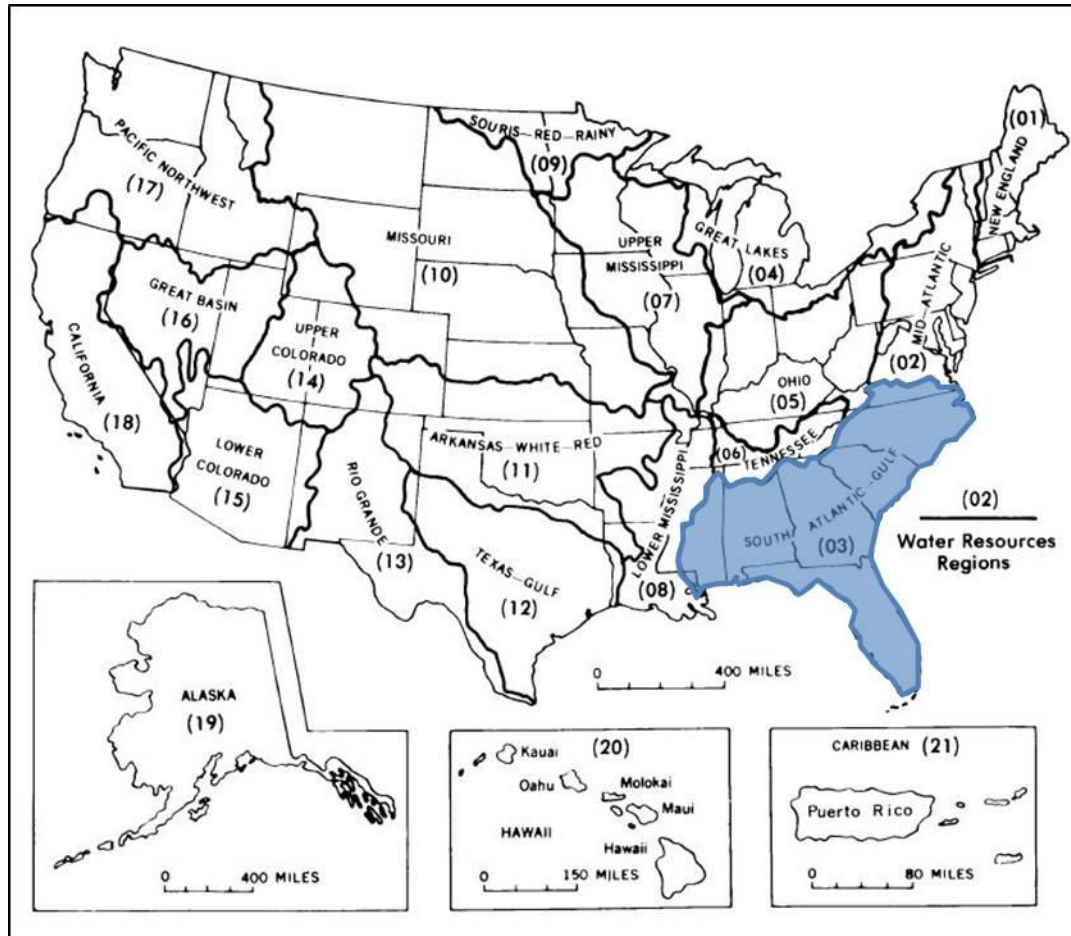


**Figure 1: USGS HUC Regions in the U.S. (Seaber *et al.*, 1987)**

HUC region 03 is the South Atlantic-Gulf region (shown in blue in Figure 1), in which all drainage ultimately discharges into a) the Atlantic Ocean within and between the states of Virginia and Florida; b) the Gulf of Mexico within and between the states of Florida and Louisiana; and c) the associated waters. HUC region 03 includes all of Florida and South Carolina, and parts of Alabama, Georgia, Louisiana, Mississippi, North Carolina, Tennessee, and Virginia, and has a total area of 721,520 square kilometers.

### **1.3 Climate Oscillations and Streamflow Extremes**

A teleconnection is a strong statistical relationship between weather in different parts of the globe. Pressure, circulation, and temperature anomalies occur thousands of kilometers away from each other, yet they are related (Pierce, 2013). One such example of a teleconnection is the link between sea surface temperature (SST) and weather in other parts of the globe. Regular shifts in SST and pressure from one state to another are known as oscillations (Earth Gauge, 2015). The length of these oscillations can range from interannual to multidecadal timescales. Additionally, oscillations have different effects over different geographic locations (Pierce, 2013). Understanding the effects and nature of various oscillations will help communities and land and resource managers understand local and regional implications, anticipate effects, and prepare for changes (USGS, 2007).

#### **1.3.1 Climate Oscillations**

This study will investigate the influences of four oceanic-atmospheric modes of variability: El Niño-Southern Oscillation (ENSO), the Pacific Decadal Oscillation (PDO), the Atlantic Multidecadal Oscillation (AMO), and the North Atlantic Oscillation (NAO). These climate oscillations have very different timescales, and all of them alternate between warm/positive and cool/negative phases. In the event of overlap between oscillations, they will either exaggerate or obscure each other's effects.

#### **1.3.2 Streamflow Extremes**

Climate variability affects all aspects of hydrology and water resources through the water budget. An issue of critical concern to the water-resource planning and management communities is low flows and droughts. The characteristics of low flows in

rivers and streams are important metrics for water managers who must meet a growing number of water-supply requirements, particularly when low flows persist over an extended period as during drought. Low flows are also critical for managing water quality where pollutant concentrations must be maintained below regulatory thresholds required by the Clean Water Act (Lins *et al.*, 2010).

### **1.3.3 Oceanic-Atmospheric Influences on Streamflows**

The goal of the research presented in this thesis is to improve the understanding of how large-scale ocean-atmosphere phenomena influence streamflow extremes in southeastern United States, especially lower-end extremes. To attain the research goal, parametric and nonparametric testing was utilized to evaluate the influences of alternating phases of ENSO, PDO, AMO, and NAO on streamflows.

### **1.4 Problem Statement**

A climate oscillation is a periodic shift in sea surface temperature and pressure as a result of a teleconnection. There are 4 major atmospheric-oceanic oscillations that affect the study area of southeastern United States: ENSO, PDO, AMO, and NAO. These climate oscillations have significant effects on streamflow extremes, including lower-end extremes such as low flows and droughts. However, there is considerable spatial and temporal variability of influences between these oscillations. Thus, detailed spatial and temporal analysis of streamflow extremes is necessary to determine whether certain areas are more susceptible to low flows or drought conditions under alternating phases of these oscillations.

## 1.5 Objectives of the Study

This thesis analyzes the influences of atmospheric-oceanic oscillations on streamflow extremes in southeastern United States. Several low flow indices are analyzed during the warm and cool phases of ENSO, PDO, AMO, and NAO. Parametric and nonparametric tests are used to evaluate statistically significant differences in streamflow extremes. The main objectives are:

- 1) Understand the spatial and temporal variability of low flows under two phases of interannual, decadal, quasidecadal, and multidecadal oscillations on a regional scale.
- 2) Assess the spatial variability of streamflow extremes under two phases of oscillations using flow duration curves.
- 3) Determine and compare low-flow frequency statistics using annual 7-day average minimum flows for two phases of oscillations.
- 4) Calculate the 7Q10 and assess the spatial variability of this low flow index under two phases of oscillations.
- 5) Apply parametric statistical tests to the 7Q10 low flow index to determine if statistically significant differences in low flow extremes exist between two phases of oscillations.
- 6) Use the occurrences of low flows to determine the temporal differences between two phases of oscillations.
- 7) Analyze the differences between the streamflow deficit durations for the two phases of oscillations.

## **1.6 Thesis Organization**

The contents of this thesis are organized as follows:

Chapter 1: Introduces the study domain and briefly discusses climate oscillations as well as low flows/droughts. Discusses the main objectives of the study.

Chapter 2: A literature review of the major oscillations that are known to affect precipitation and streamflow in southeastern United States (ENSO, PDO, AMO, NAO). Discusses methods of analysis and results from similar studies.

Chapter 3: Outlines the methodology used to evaluate streamflow extremes and characteristics. Includes low-flow frequency analysis, streamflow deficit, and flow duration curve as well as the parametric and non-parametric tests that were used in the analysis.

Chapter 4: The methodology described in Chapter 3 is applied for analysis at 43 stations in the case study area. Further details of data collection and processing are presented as well.

Chapter 5: The results of the thesis are analyzed and presented.

Chapter 6: The conclusion of the study is presented, along with the contribution and limitations of the study, and recommendations for further research.

## **2 LITERATURE REVIEW**

### **2.1 Oceanic-Atmospheric Variability**

There are several major oscillations which are known to affect the precipitation and streamflow patterns in southeastern United States. The focus of this study will include the following: El Niño-Southern Oscillation, Pacific Decadal Oscillation, Atlantic Multidecadal Oscillation, and North Atlantic Oscillation.

#### **2.1.1 El Niño-Southern Oscillation (ENSO)**

Under normal atmospheric conditions, there is a persistent high pressure zone that exists along the eastern South Pacific and an equally persistent low pressure zone that exists along the western South Pacific. Typically, there is cool water in the eastern region and warm water in the western region. The southeast trade winds are driven by the differences in atmospheric pressure and they tend to move water westward along the equator, keeping warm sea surface temperatures (SST) in the western equatorial Pacific (Coley and Waylen, 2006). However, in periods ranging from two to seven years, atmospheric pressure will oscillate across the South Pacific such that the pressure over the western Pacific becomes anomalously high while the pressure over the eastern Pacific becomes anomalously low (Zorn and Waylen, 1997). This is known as the Southern Oscillation.

The warm water in the western South Pacific is a major source of atmospheric heating that drives large scale convection circulation patterns (Coley and Waylen, 2006).

When the Southern Oscillation enters into a negative phase, the strength of the trade winds is diminished, allowing the warmer sea surface temperatures to migrate eastward. This releases heat to the atmosphere (in the form of moisture) and disrupts circulation patterns. This situation, of increasing sea surface temperature and atmospheric moisture migrating eastward, represents an El Niño event (Coley and Waylen, 2006). La Niña refers to times when the “typical” condition is intensified, i.e. when colder than normal waters exist in response to anomalously high atmospheric pressure across the eastern South Pacific. Taken together, the oceanic-atmospheric interaction of see-sawing pressures and temperatures is referred to as the El Niño-Southern Oscillation (ENSO).

Currently, there is no single data set that is universally accepted for distinguishing between warm and cool ENSO episodes. For this report, the methodology adapted by Goly and Teegavarapu (2014) is used. ENSO events are categorized as El Niño (La Niña) when the seasonal mean of Niño 3.4 sea surface temperature anomalies is greater than  $+0.5\text{ }^{\circ}\text{C}$  ( $-0.5\text{ }^{\circ}\text{C}$ ). A complete list of El Niño and La Niña years used in this study is provided in the case study chapter.

### **2.1.2 Pacific Decadal Oscillation (PDO)**

The Pacific Decadal Oscillation (PDO) is an oceanic-atmospheric phenomenon associated with persistent, bimodal climate patterns in the northern Pacific Ocean. The PDO oscillates with a characteristic period on the order of 50 years, with a particular phase of the PDO typically lasting about 25 years (Tootle *et al.*, 2005). Changes in Pacific climate have widespread impacts on natural systems, including water resources in the Americas and many marine fisheries in the North Pacific (Mantua and Hare, 2002).

During the warm phase of PDO, SSTs are anomalously cool in the central North Pacific and anomalously warm along the west coast of the Americas. Additionally, low pressure anomalies occur in the North Pacific causing enhanced counterclockwise winds, while high pressure anomalies in the northern subtropical region cause enhanced clockwise winds (Mantua and Hare, 2002). Anomalous climate conditions associated with the warm phases of PDO (SST, sea level pressure, and surface wind) are shown in Figure 2.

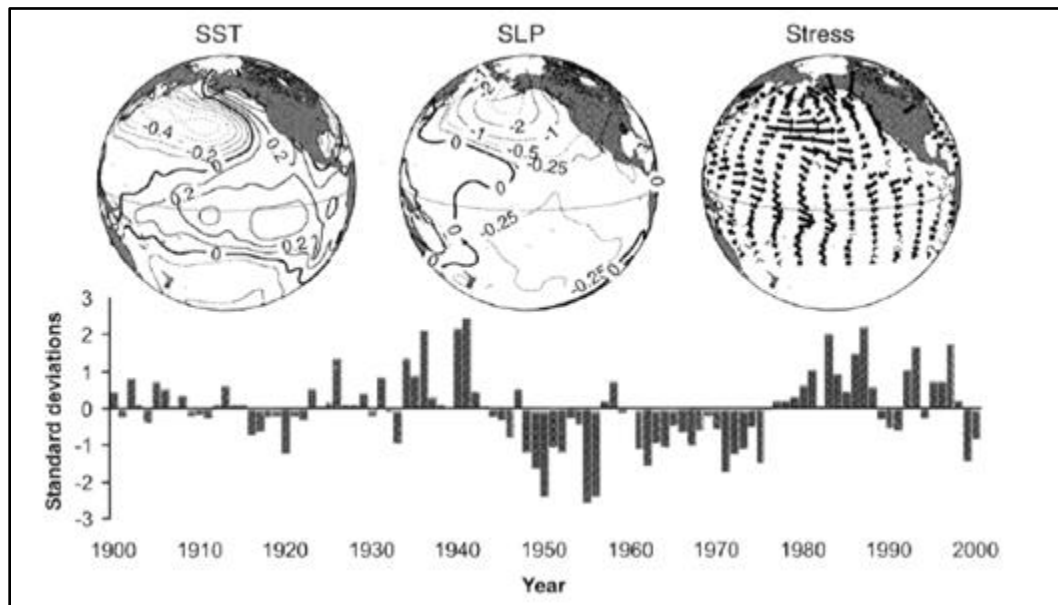


**Figure 2: Anomalous Climate Conditions Associated with Warm Phase PDO**  
(Mantua and Hare, 2002)

For this study, the PDO index values established by Tootle *et al.* (2005) were used to differentiate between the warm and cool phases of the PDO. These values were established by the Joint Institute for the Study of the Atmosphere and Ocean at the University of Washington. The temporal windows for the warm and cool phases of PDO are outlined in the case study chapter.



### 2.1.3 Atlantic Multidecadal Oscillation (AMO)

The Atlantic Multidecadal Oscillation (AMO) is a pattern of Atlantic climate variability which is detected as a fluctuation in SSTs over the Atlantic Ocean, between the equator and Greenland (Goly and Teegavarapu, 2014). The geographical location of where SST anomalies are calculated is shown in Figure 3.

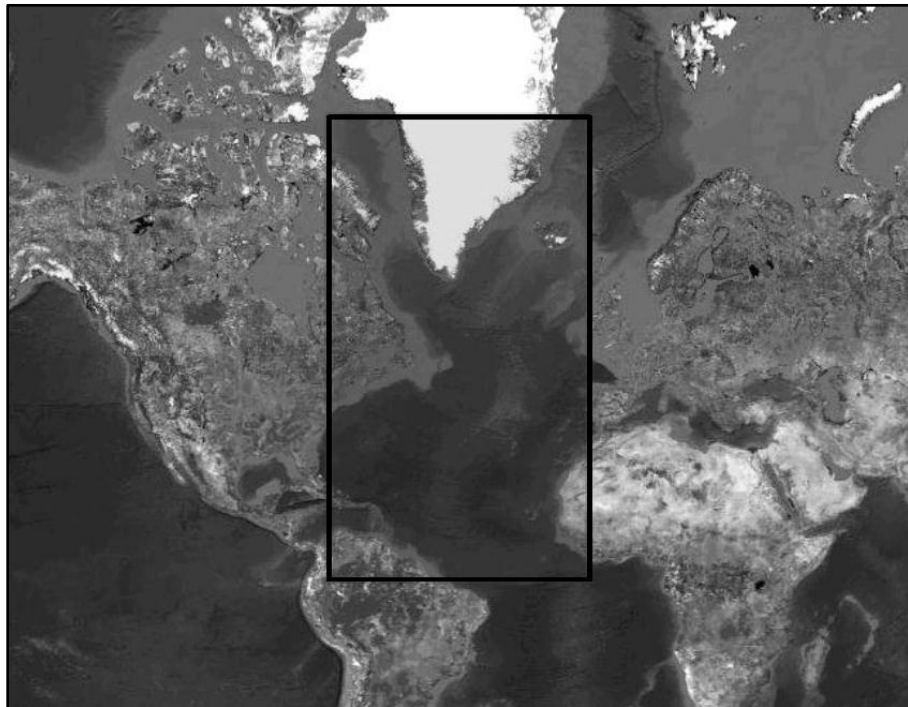


**Figure 3: Spatial Coverage of AMO Influence (Pierce, 2013)**

AMO is a long-range climatic oscillation that causes periodic changes in the surface temperature of the Atlantic Ocean, which persists for around 20 – 40 years (Goly and Teegavarapu, 2014). For this report, the AMO index used by Goly and Teegavarapu (2014) is adopted to define the warm and cool phases of AMO and is outlined in the case study chapter.

#### 2.1.4 North Atlantic Oscillation (NAO)

A major source of variability in the atmospheric circulation is the North Atlantic Oscillation (NAO), which is associated with changes in the surface westerlies across the North Atlantic onto Europe (Hurrell, 1995). NAO refers to a meridional oscillation in atmospheric mass with centers of action near the Icelandic low and the Azores high (Hurrell and Van Loon, 1997). While it is evident throughout the year, it is most pronounced during winter. A simple index of the NAO can be defined as the difference between the normalized mean winter sea level pressure anomalies at Lisbon, Portugal and Stykkisholmur, Iceland and is shown in Figure 4.

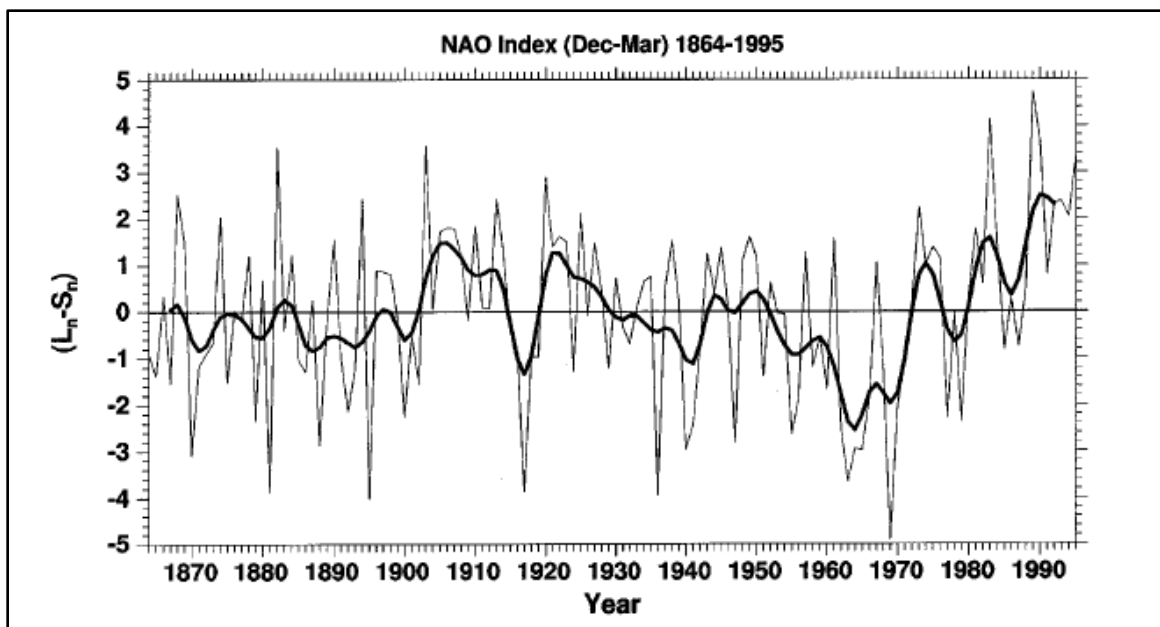


**Figure 4: NAO Index 1864 – 1995 (Hurrell and Van Loon, 1997)**

Positive values of the index indicate stronger-than-average westerlies over the middle latitudes associated with low pressure anomalies over the region of the Icelandic low and high pressures anomalies across the subtropical Atlantic (Hurrell and Van Loon,

1997). Using the NAO index values established by Tootle *et al.* (2005), the positive and negative phases of the NAO are outlined in the case study chapter.

## **2.2 Methods of Analysis**

There have been many studies investigating the influences of oceanic-atmospheric oscillations on hydrologic variables. Typically, the first step in the analysis is to index each year in the period of record as warm or cool for whichever oceanic-atmospheric oscillation is being studied. Next, a test is used to determine whether the two independent data sets (e.g., data from AMO warm and cool phases) are significantly different. This method of analysis has been applied to different hydrologic variables including precipitation (Teegavarapu *et al.*, 2013; Goly and Teegavarapu, 2014), streamflow (Rogers and Coleman, 2003; Zorn and Waylen, 1997; Tootle *et al.*, 2005), or both (Schmidt *et al.*, 2001).

### **2.2.1 Precipitation Extremes and Variations**

Teegavarpu *et al.* (2013) studied the influence of AMO on precipitation extremes in Florida. They found that there is an increase in precipitation extremes in warm phases of AMO for durations greater than 24 hours. They also found that the influence of warm or cool phase on AMO on precipitation extremes is not spatially uniform in the region. Additionally, the authors found that there is a temporal shift in the occurrences of the extremes from the later part of the year in warm phases to earlier in the year for cool phases.

Goly and Teegavarpu (2014) studied the individual and coupled influences of AMO and ENSO on precipitation extremes and characteristics in Florida. They found that the

AMO influences vary between the peninsular and continental parts of Florida and that the warm (cool) phase of AMO contributes to increased precipitation extremes during the wet (dry) season. The effects of ENSO were also limited to the dry season, with El Niño (La Niña) causing an increase (decrease) in extremes and total precipitation.

Schmidt *et al.* (2001) studied ENSO influences on seasonal precipitation totals in Florida. For winter months, total seasonal precipitation showed strong responses to ENSO phase. Statewide, El Niño (La Niña) winter precipitation totals were higher (lower) than during neutral winters. For spring, the response to ENSO phase did not change dramatically: only 11% of stations had significantly higher levels of precipitation for El Niño springs and only 13% of stations had significantly lower levels of precipitation for La Niña springs. For the summer, Florida experienced its highest precipitation levels, but this pattern did not change for El Niño or La Niña years. For the fall, 57% of stations received significantly higher rainfall during El Niño falls and 65% of stations received significantly less rainfall during La Niña falls.

### **2.2.2 Streamflow Variations**

Rogers and Coleman (2003) studied winter streamgauge data to evaluate interactions between the AMO, the Pacific/North American teleconnection pattern (PNA), and ENSO events in producing Mississippi River basin discharge variations. The most consistent eastern U.S. AMO winter signal occurs in the upper Mississippi River basin, producing low (high) streamflow during its warm (cool) phase. However, the authors found that this was not true for the lower Mississippi basin. During the late 1940s and early 1950s, despite being in the core AMO positive phase, the lower Mississippi basin experienced

heavy rain and discharges. The authors discovered that these anomalous winters were caused by significant responses to ENSO and the PNA.

Zorn and Waylen (1997) studied the response of mean monthly streamflow to ENSO in north central Florida. The region selected experiences streamflow maximums in both the winter (from frontal systems in the panhandle region) and the summer (from convectional and tropical storms in the southern region). The authors found that winter season discharge peaks in February for cold events, but is maintained through March and April for warm events. Thus, there is a tendency for the winter peak to be both greater in magnitude and longer in duration during warm years. For the summer, it was found that the duration of the summer seasonal peak in streamflow was similar for both warm and cold years. However, there is a statistically significant difference in variability in streamflow during cold events compared to warm events. This suggests that there is likely to be a larger summer peak in streamflow during colder years with wider variation about the mean.

Tootle *et al.* (2005) studied coupled influences of four modes of variability (ENSO, PDO, AMO, NAO) on streamflow across the continental U.S. Their study was a comprehensive investigation of large regions to investigate whether ocean atmosphere phenomena influence hydrology at a large scale both individually (PDO, AMO, NAO, ENSO) and coupled modes with ENSO (PDO/ENSO, AMO/ENSO, NAO/ENSO).

For PDO, there were two distinct regions in which there was a significant difference in streamflow between warm phase and cool phase: upper to middle Mississippi River basin and Southwest. Both exhibited greater streamflow in PDO warm phase than PDO

cool phase. Four regions were identified as having significant differences between warm phase and cool phase of AMO: Pacific Northwest, upper to middle Mississippi River basin, lower Appalachians/Gulf of Mexico, and Southwest. The Pacific Northwest is a negative region, i.e., AMO warm phase results in increased streamflow compared to AMO cool phase. The remaining three regions are positive, so the opposite is true. There is one region in the continental U.S. which was identified as having a significant difference in NAO negative and NAO positive phase. For the upper to middle Mississippi River basin the NAO positive phase results in increased streamflow compared to the NAO negative phase. ENSO signals were displayed in three regions: Florida, the Southwest, and the Pacific Northwest. Strong negative (i.e., El Niño resulted in increased streamflow when compared to La Niña) for Florida and the Southwest while the opposite was true for the Pacific Northwest.

The coupling of PDO and ENSO was evaluated by examining the streamflow relationships for PDO cool/El Niño, PDO warm/El Niño, PDO cool/La Niña, and PDO warm/La Niña. At the 95% significance level, the authors did not identify a PDO impact of ENSO. The coupling of AMO and ENSO was evaluated by examining the streamflow relationships for AMO cool/El Niño, AMO warm/El Niño, AMO cool/La Niña, and AMO warm/La Niña. There are significant differences in streamflow for AMO cool/La Niña and AMO warm/La Niña in the Southeast. In the Southeast region of the United States, a La Niña event generally results in decreased streamflow while the AMO cool (warm) phase results in increased (decreased) streamflow. Therefore, La Niña events occurring in an AMO cool (warm) phase results in significantly greater (lesser) streamflow than those occurring in an AMO warm (cool) phase. Essentially, a La Niña

during the AMO warm phase results in more severe droughts. The coupling of NAO and ENSO was evaluated by examining the streamflow relationships for NAO negative/El Niño, NAO positive/El Niño, NAO negative/La Niña, and NAO positive/La Niña. For NAO negative/La Niña and NAO positive/La Niña, the Midwestern region of the United States was found to have significant streamflow differences. A La Niña that occurs during an NAO positive phase results in significantly more streamflow than a La Niña during an NAO negative phase.

This thesis differs from previous research in several key areas. Most importantly, this thesis focuses specifically on low flows. Whereas previous research typically evaluated streamflow means and medians, this study will investigate several low-flow regime measures as outlined by the World Meteorological Organization Manual on Low-Flow Estimation and Prediction (World Meteorological Organization, 2008). Additionally, this thesis will study the effects of 4 of the major oceanic-atmospheric oscillations that affect hydrologic variables in this study area: ENSO, PDO, AMO, and NAO. Finally, this study utilizes only high quality streamflow data from the USGS Hydro-Climatic Data Network so that results will not have been confounded by anthropogenic activity.

### 3 METHODS OF ANALYSIS

The methods used to evaluate streamflow extremes and characteristics are explained in this chapter. A visual illustration of the procedures used in the methodology is shown in Figure 5.

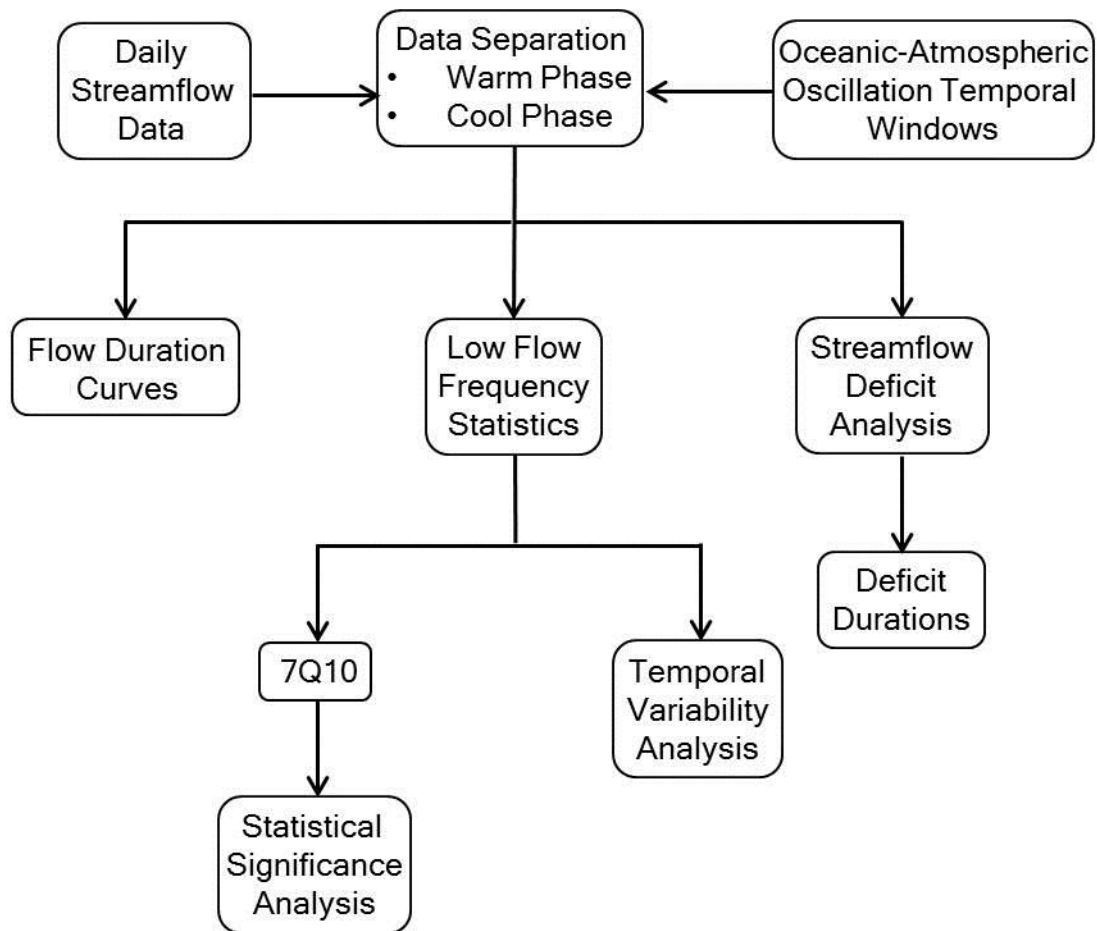


**Figure 5: Methodology for Evaluation of Trends in Streamflow Extremes and Climate Variability**



The first step in the methodology is to separate the daily streamflow data into warm and cool phases using the temporal windows for each oscillation. Once this is done the following analyses were performed on the two phases of each oscillation: flow duration curves, low flow frequency statistics, and streamflow deficit analysis. These analyses will be discussed in greater detail in the following sections.

### 3.1 Flow Duration Curves

A flow duration curve (FDC) is one of the most informative methods of displaying the complete range of river discharges. It is the relationship between any given discharge value and the percentage of time that this discharge is equaled or exceeded (Smakhtin, 2001). A FDC was constructed for the warm and cool phase for each station by ranking the daily discharges and calculating the frequency of exceedance for each value. Doing so effectively reorders the observed hydrograph by one ordered by time to one ordered by magnitude (Hisdal and Gustard, 2008).

The FDC was determined by following the following steps:

- 1) Use the mean discharge values ( $Q$ ) for the whole period of record. The total number of days and streamflow values are ( $n$ ).
- 2) Calculate the rank ( $m$ ) of each value by sorting the values in ascending order (the lowest discharge has rank 1 and highest discharge has rank  $n$ ).
- 3) Calculate the exceedance probability ( $EP$ ) using the following equation:

$$EP = 1 - \frac{m}{n+1} \quad (1)$$

- 4) Tabulate and sort the corresponding values of streamflow ( $Q_m$ ) and exceedance probability ( $EP_m$ ).

- 5) Plot the FDC. The X-axis is the exceedance probability and the Y-axis is the streamflow. The streamflow axis is logarithmic to enable a wide range of flows to be plotted and ensures that the low-flow range is clear on the graph (Hisdal and Gustard, 2008).

One FDC was created for each station for every oscillation. The FDC created included both phases of the oscillation plotted on top of the other to visually determine which phase had the lower flow for a given exceedance probability.

### **3.2 Low Flow Frequency Analysis**

Low flow frequency indices are widely used in drought studies, design of water supply systems, estimation of safe surface water withdrawals, classification of streams' assimilative capacity for waste, etc. (Smakhtin, 2001). For this report, the 7-day average minimum value (AM7) was determined for each year in the period of record for the warm and cool phases of each oscillation. The AM7 is the average flow measured during the 7 consecutive days of lowest flows during any given year (Nnaji *et al.*, 2014). In section 3.2.1, the AM7 values were used to estimate the 7Q10 low flow index. In section 3.2.2, the 7Q10 values were tested for significant difference between the warm and cool phase of each oscillation. In section 3.2.3, the temporal occurrences of AM7 values were investigated.

#### **3.2.1 Estimates of 7Q10 Low Flow Index**

Estimates of the probability of occurrence of low-flow events can be derived from historical records using frequency analysis (Tallaksen and Hewa, 2008). The most widely used index of low flow in the United States is the 7Q10 method developed by the USGS.

This is defined as the lowest 7-day average flow that occurs on average once every 10 years. Estimation of the 7Q10 from streamflow records consists of determining a probability distribution of the AM7 values and selection of a statistically efficient parameter-estimating procedure (Nnaji *et al.*, 2014). For this report, AM7 values for the period of record for each station were fitted to the Weibull distribution, as shown in Equation 2 (Gumbel, 1958).

$$F(x) = 1 - \exp\left[-\left(\frac{x-\lambda}{\alpha}\right)^k\right] \quad (2)$$

Where  $k$ ,  $\alpha$ , and  $\lambda$  are the shape, scale, and location parameters, respectively. The parameters of the Weibull distribution were estimated by the Maximum Likelihood Estimation (MLE) method. The goodness-of-fit of the Weibull distribution to the data set was tested using the Kolmogorov-Smirnov (KS) test as well as the Chi-Square test. If both tests passed, only then was the 7Q10 calculated.

The 7Q10 was determined for each station using the following steps:

- 1) Determine AM7 for each year in the period of record. The total number of values is ( $n$ ).
- 2) Calculate the rank ( $m$ ) of each AM7 value by sorting the values in ascending order (the lowest value has rank 1 and the highest value has rank  $n$ ).
- 3) Calculate the non-exceedance probability (NEP) using the following equation:

$$NEP = \frac{m}{n+1} \quad (3)$$

- 4) Tabulate and sort the corresponding values of 7-day average minimum values ( $AM7_m$ ) and non-exceedance probability ( $NEP_m$ ).

- 5) Plot the non-exceedance probability. The X-axis is the AM7 and the Y-axis is the non-exceedance probability.
- 6) Fit the data with a Weibull distribution (parameters estimated by the MLE method) using MATLAB.
- 7) Test the goodness-of-fit using the KS test. This is a nonparametric hypothesis test that evaluates the maximum absolute difference between the non-exceedance probability distribution and the Weibull distribution.
- 8) Test the goodness-of-fit using Chi-Square test. This test determines if a data sample comes from a specific probability distribution with parameters estimated from the data. The test groups the data into bins, calculating the observed and expected counts for each bin, and computes the Chi-Square test statistic.
- 9) If the Weibull distribution passes both tests, determine the 7Q10 value, i.e., the annual minimum 7-day flow value in which  $NEP = 0.1$ .

### **3.2.2 7Q10 Statistical Significance Analysis**

To determine whether there is a statistical significance between the 7Q10 values for warm and cool phases, parametric tests were used. The two-sample unpaired t-test is a parametric test that is performed on the response of streamflow to changes in oceanic-atmospheric phase. This test compares two data sets and determines if one data set has significantly lower values than the other. There are several variations on the t-test:

- 1) Data may be either paired or unpaired. Unpaired data indicates that the two samples (e.g., warm phase and cool phase) have no connection and are independent.

- 2) The variances of the two samples may be either equal or unequal. Either may be used in the t-test; however, different formulas are used for each.

Additionally, parametric tests require that the data be normally distributed. The normality of the data sets is first confirmed using visual checks (histograms, normal probability plots, etc.). Statistical tests including Lilliefors (Lilliefors, 1967), Jarque-Bera (Jarque and Bera, 1987) and Chi-Square goodness-of-fit (Corder and Foreman, 2009) were also used to confirm normality. In cases where the raw data sets did not conform to normality, Box-Cox transformation (Box and Cox, 1964) was used. Box-Cox transformation is a commonly used power transformation that uses the parameter ( $\lambda$ ), shown in Equation 4, to change the shape of the data distribution to nearly symmetric (Wilks, 2011).

$$T(x) = \begin{cases} \frac{x^\lambda - 1}{\lambda}, & \lambda \neq 0 \\ \ln(x), & \lambda = 0 \end{cases} \quad (4)$$

After the data is normally distributed, the two-sample F test is used to evaluate the sample variances. Finally, after the normality has been confirmed and the variances have been determined, the two-sample t-test is performed. This test is a hypothesis test: the null hypothesis indicates that the two independent samples, both coming from normal distributions, are equal. If the null hypothesis is rejected, then the streamflow responses for warm and cool phases for a given climatic oscillation are statistically different.

### 3.2.3 Temporal Variability Analysis

An important factor in analyzing streamflow extremes is the temporal distribution of occurrences throughout the year, as well as the variation between the phases. The

knowledge of the timing of low flows is extremely valuable for water resources management. In this study, Kernel density estimates (KDE) were utilized to study the occurrence of extremes for the warm and cool phases of all oscillations. KDE is a non-parametric method that displays a smooth curve to show the distribution of the occurrences of extremes throughout the year. Histograms can also convey similar information; however, the KDE will not be influenced by the location and the number of bins making KDE a better visual tool in comparative assessment of temporal occurrences of the extremes (Pierce, 2013). The following steps were taken for the warm and cool phase for each station:

- 1) Determine the AM7 value for each year in the period of record.
- 2) Determine the month in which the AM7 value occurs. Months are denoted as 1 through 12 for January to December, respectively.
- 3) Evaluate the temporal occurrences of AM7 using KDE plots.

### **3.3 Streamflow Deficit**

Streamflow deficit analysis is widely used for the identification, characterization, and management of multiyear hydrological droughts. The type of information obtained from this analysis is used for different purposes: domestic water supply, irrigation, power generation, dilution of industrial pollutants, etc., which are all dependent on the continuous availability of prescribed river discharges (Smakhtin, 2001).

A streamflow deficit occurs when the river is below a specific threshold that defines a drought or critical deficit. The deficit starts when the flow goes below the threshold and

ends as soon as the flow returns above the threshold. In Figure 6 the definition of timing, duration, and volumes of deficits below a threshold discharge in a river is shown.

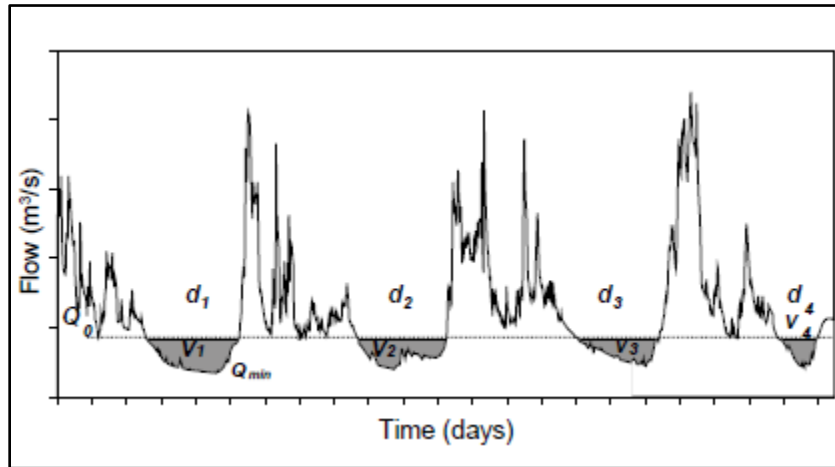


**Figure 6: Definition of Deficit Characteristics (Hisdal, 2008)**

For this report, the deficit duration will be determined for the warm and cool phase for each oscillation. Cumulative probability plots of the deficit durations were created for each station to determine if longer deficit durations were most likely to occur during the warm or cool phase of an oscillation. The following steps were taken for this analysis:

- 1) Plot the streamflow hydrograph for the entire period of record.
- 2) Select the deficit threshold. A sequence of deficit events is obtained from the streamflow hydrograph by considering periods with flow below a certain threshold. The threshold for all stations will be  $Q_{95}$ , i.e., the flow which is equaled or exceeded 95% percent of the time.
- 3) Determine the total deficit duration (days) for the period of record for the warm and cool phases.

- 4) Create a cumulative probability plot (i.e., a non-exceedance probability plot) using the deficit duration values for the warm and cool phase for each station by following the following steps.
- 5) Calculate the rank ( $m$ ) of each deficit duration value ( $DD$ ) by sorting the values in ascending order (the lowest value has rank 1 and the highest value has rank  $n$ ).
- 6) Calculate the non-exceedance probability using Equation 3 described previously.
- 7) Tabulate and sort the corresponding values of deficit duration values ( $DD_m$ ) and non-exceedance probability ( $NEP_m$ ).
- 8) Plot the non-exceedance probability. The deficit duration values are the X-axis and the non-exceedance probability is the Y-axis.



## 4 STUDY DOMAIN

### 4.1 Study Region

The study domain for this thesis is the southeastern United States, specifically HUC region 03. It has a total area of 721,520 square kilometers and occupies the following states: Florida, South Carolina, Alabama, Georgia, Louisiana, Mississippi, North Carolina, Tennessee, and Virginia. This region is bounded by the Gulf of Mexico and the Atlantic Ocean.

The Köppen-Geiger climate classification system is used to differentiate between different climates within the study domain. This method uses a three-letter system: the first letter indicates the zone (equatorial, arid, warm temperate, snow, polar), the second letter considers the precipitation (desert, steppe, fully humid, summer dry, winter dry, monsoonal), and the third letter considers the temperature (hot arid, cold arid, hot summer, warm summer, cool summer, extremely continental, polar frost, polar tundra) (Kottek *et al.*, 2006). The majority of the study area is warm temperate, fully humid, and hot summer (Cfa). There is some variation in south Florida: the southernmost area of the state is equatorial, winter dry (Aw) and a section on the east coast is equatorial, monsoonal (Am). There is also a small area in the northeast section of the study domain that is warm temperate, fully humid, and cool summer (Cfc). The different climate regions within the study domain are shown in Figure 7.

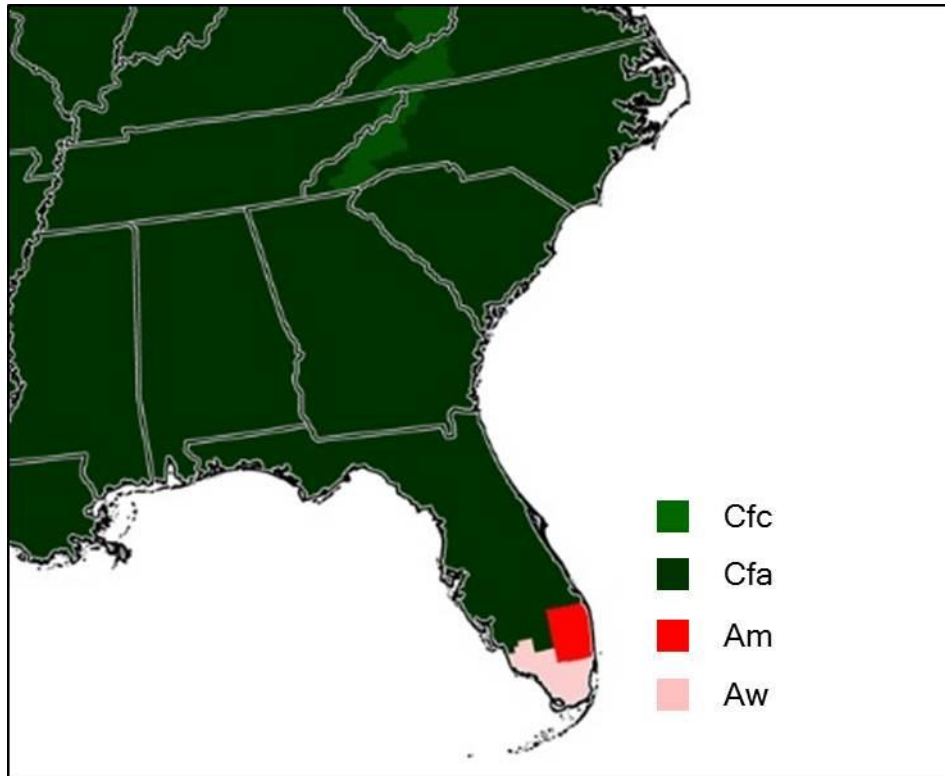


**Figure 7: Climate Regions within HUC Region 03 Based on the Köppen-Geiger Climate Classification (Kottek *et al.*, 2006)**

## 4.2 Data Sets

The two major data sets used to develop the relationships between oceanic-atmospheric variability and streamflow extremes are unimpaired streamflow data for the southeastern United States and oceanic-atmospheric data for the Pacific and Atlantic Oceans.

### 4.1.1 Streamflow Data

While surface-water conditions are generally correlated with fluctuations in meteorologic variables (such as precipitation and temperature), the dynamics of

streamflow are not just a simple first-order response to existing atmospheric conditions and meteorologic fluxes. Inputs from diverse specific precipitation events are collected over the surface of the watershed so that the meteorologic events are spatially integrated by the watershed. Meteorologic events are also temporally integrated because the watershed retains moisture both on and below its surface. Thus, the watershed acts to dampen the noisy signal of specific instantaneous and local meteorologic events. Records of streamflow can provide a filtered account of prevailing climatic conditions over the watershed (Slack and Landwehr, 1992).

The ability of streamflow records to reflect variations in the prevailing climate is conditioned on the absence of any other major causes that would radically alter streamflow patterns during the period of record. Such confounding processes would generally be anthropogenic in origin. Human actions can affect streamflow patterns directly, such as the removal of water from a stream for consumptive use, or indirectly, by changing the watershed storage capacity due to land-use changes during the period of record. In either case, the pattern of past climate variation to be discerned in the streamflow record would be confounded by changes induced by anthropogenic activity (Slack and Landwehr, 1992). In this thesis, sites included in the USGS Hydro-Climatic Data Network (HCDN) were used for analysis. The HCDN is a subset of all USGS streamgages which have relatively long streamflow records that are predominantly free of anthropogenic influences. The purpose of the network is to provide a streamflow dataset suitable for analyzing the hydrologic variations and trends in a climatic context (Lins, 2012).

Mean daily discharges at 43 USGS stations were ultimately selected to be analyzed. The streamflow data station list is summarized in Tables 1 and 2. To be selected the stations had to meet the following criteria:

- 1) Stations were included in the USGS HCDN.
- 2) Stations were located within USGS HUC region 03.
- 3) Stations had at least 50 years of continuous streamflow data through 2013.

**Table 1: Case Study Streamflow Data Station List (Part 1)**

<b>Station Number*</b>	<b>Station ID</b>	<b>Station Name</b>	<b>Drainage Area (km<sup>2</sup>)</b>	<b>Latitude<sup>+</sup></b>	<b>Longitude<sup>+</sup></b>
1	2046000	Stony Creek near Dinwiddie, VA	288.5	37.067094	-77.602489
2	2051500	Meherrin River near Lawrenceville, VA	1428.7	36.716814	-77.831658
3	2053200	Potecasi Creek near Union, NC	583.7	36.370833	-77.025556
4	2053800	S F Roanoke River near Shawsville, VA	280.7	37.140132	-80.266433
5	2055100	Tinker Creek near Daleville, VA	30.5	37.417633	-79.935319
6	2059500	Goose Creek near Huddleston, VA	485.4	37.173200	-79.520308
7	2064000	Falling River near Naruna, VA	427.8	37.126810	-78.959737
8	2065500	Cub Creek at Phenix, VA	252.6	37.079311	-78.763618
9	2069700	South Mayo River near Nettleridge, VA	221.1	36.570971	-80.129493
10	2070000	North Mayo River near Spencer, VA	270.6	36.568194	-79.987265
11	2074500	Sandy River near Danville, VA	288.5	36.619583	-79.504193
12	2081500	Tar River near Tar River, NC	428.4	36.194167	-78.583056
13	2082950	Little Fishing Creek near White Oak, NC	460.9	36.183333	-77.876111
14	2092500	Trent River near Trenton, NC	447.6	35.064167	-77.461389
15	2108000	Northeast Cape Fear River near Chinquapin, NC	1569.5	34.828889	-77.832222
16	2110500	Waccamaw River near Longs, SC	2908.3	33.912672	-78.715017
17	2111500	Reddies River at North Wilkesboro, NC	233.7	36.175000	-81.168889
18	2118500	Hunting Creek near Harmony, NC	400.5	36.000556	-80.745556
19	2128000	Little River near Star, NC	273.5	35.387222	-79.831389
20	2143000	Henry Fork near Henry River, NC	216.7	35.684444	-81.403333
21	2143040	Jacob Fork at Ramsey, NC	66.5	35.590686	-81.567037
22	2149000	Cove Creek near Lake Lure, NC	203.9	35.423454	-82.111498

\*Number on map (Figure 9)

<sup>+</sup>Expressed in decimal degrees

**Table 2: Case Study Streamflow Data Station List (Part 2)**

<b>Station Number*</b>	<b>Station ID</b>	<b>Station Name</b>	<b>Drainage Area (km<sup>2</sup>)</b>	<b>Latitude<sup>+</sup></b>	<b>Longitude</b>
23	2152100	First Broad River near Casar, NC	155.0	35.493056	-81.682222
24	2177000	Chattooga River near Clayton, GA	526.8	34.813981	-83.305993
25	2231000	St. Marys River near Macclenny, FL	1748.4	30.358847	-82.081501
26	2236500	Big Creek near Clermont, FL	146.9	28.447782	-81.740076
27	2245500	South Fork Black Creek near Penney Farms, FL	348.4	29.979408	-81.852043
28	2246000	North Fork Black Creek near Middleburg, FL	451.1	30.113295	-81.906492
29	2296500	Charlie Creek near Gardner, FL	886.4	27.375043	-81.796471
30	2297310	Horse Creek near Arcadia, FL	528.4	27.199495	-81.988419
31	2312200	Little Withlacoochee River at Rerdell, FL	413.5	28.572773	-82.155363
32	2314500	Suwannee River at US 441 at Fargo, GA	3322.2	30.680556	-82.560556
33	2315500	Suwannee River at White Springs, FL	6136.3	30.325781	-82.738183
34	2324000	Steinhatchee River near Cross City, FL	791.0	29.786613	-83.321526
35	2324400	Fenholloway River near Foley, FL	176.3	30.098271	-83.471811
36	2349900	Turkey Creek at Byromville, GA	122.9	32.195556	-83.902222
37	2361000	Choctawatchee River near Newton, AL	1781.6	31.342949	-85.610491
38	2371500	Conecuh River at Brantley, AL	1292.8	31.573495	-86.251623
39	2374500	Murder Creek near Evergreen, AL	445.7	31.418500	-86.986640
40	2472000	Leaf River near Collins, MS	1927.1	31.706944	-89.406944
41	2472500	Bouie Creek near Hattiesburg, MS	789.9	31.425833	-89.414722
42	2479300	Red Creek at Vestry, MS	1144.2	30.736111	-88.781111
43	2481000	Biloxi River at Wortham, MS	249.2	30.558611	-89.121944

\*Number on map (Figure 9)

<sup>+</sup>Expressed in decimal degrees

The locations of the 43 HCDN stations used for this analysis are shown in Figure 8.

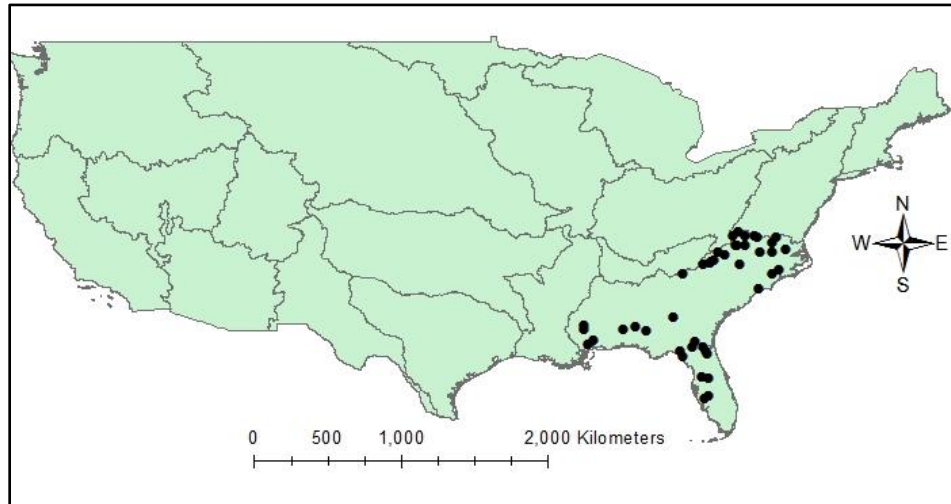


**Figure 8: HCDN Stations Used for this Study**

The stations can be roughly separated into 2 groups. Group 1 is the northern group of stations which includes stations 1 through 24 located in the states of Virginia, North Carolina, South Carolina, and north Georgia. Group 2 is the southern group which includes stations 25 through 43 located in the states of Florida, Alabama, Mississippi, and south Georgia. A closer view of the labeled stations for both groups is shown in Figure 9.

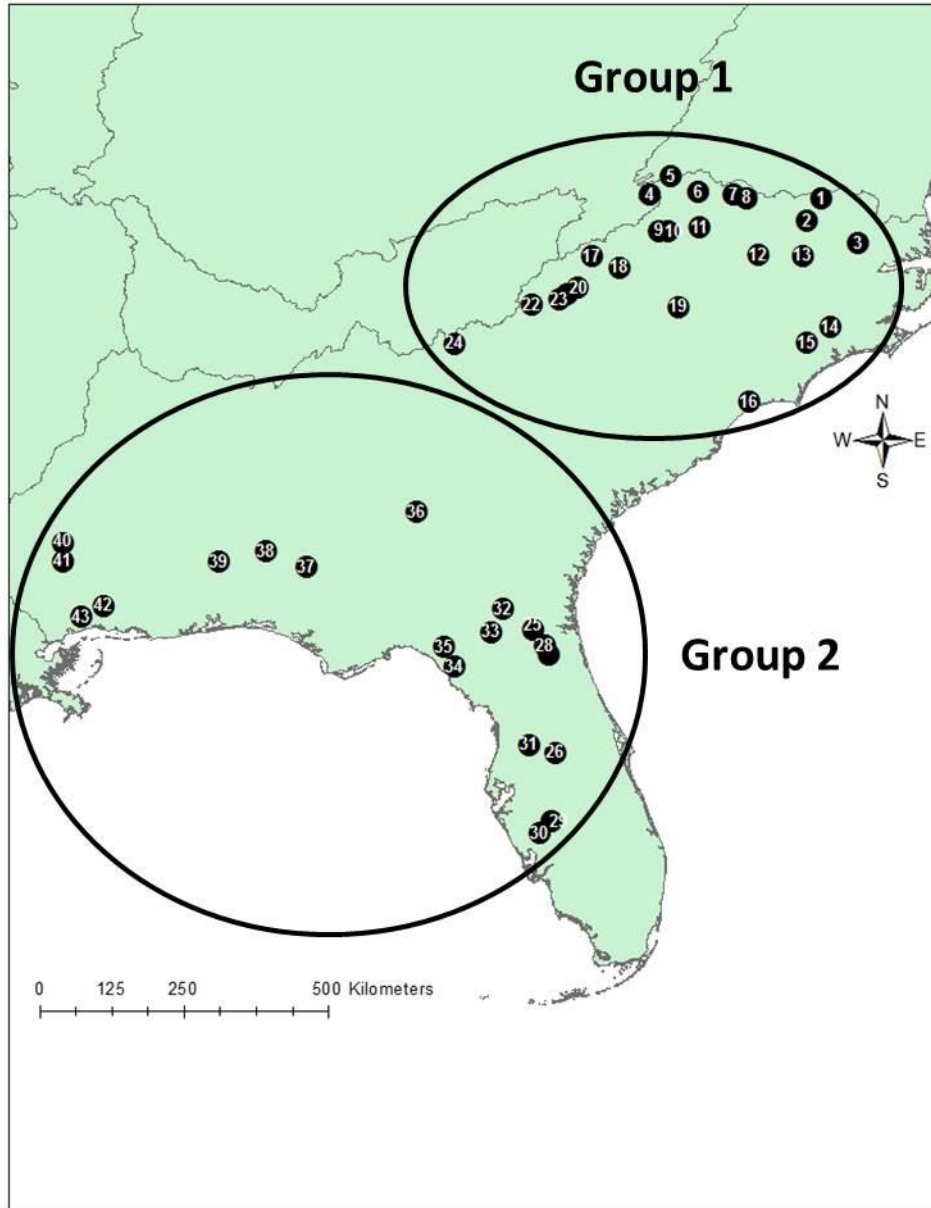


**Figure 9: HCDN Stations used for this Study Divided by Geographic Location**

#### **4.1.2 Warm and Cool Phases of Oscillations**

The temporal windows for the warm and cool phases for each oscillation were applied to the entire period of record for every station. The timescales include interannual (ENSO), decadal (PDO), quasidecadal (NAO), and multidecadal (AMO) and are



described in the literature review in Chapter 2. The lists of years for each oscillation phase are outlined in Tables 3 – 6.

**Table 3: Temporal Windows for El Niño and La Niña Phases of ENSO**

<b>Phase</b>	<b>Years</b>
El Niño	1902, 1904, 1905, 1911, 1913, 1918, 1925, 1929, 1930, 1940, 1951, 1957, 1963, 1965, 1969, 1972, 1976, 1982, 1986, 1987, 1991, 1997, 2002, 2006, 2009
La Niña	1908, 1909, 1910, 1916, 1922, 1924, 1938, 1942, 1944, 1949, 1954, 1955, 1956, 1964, 1967, 1970, 1971, 1973, 1974, 1975, 1988, 1998, 1999, 2007, 2010

**Table 4: Temporal Windows for Warm and Cool Phases of PDO**

<b>Phase</b>	<b>Years</b>
Cool	1900 – 1925
Warm	1926 – 1945
Cool	1946 – 1976
Warm	1977 – 1999
Cool	2000 – 2010

**Table 5: Temporal Windows for Warm and Cool Phases of AMO**

<b>Phase</b>	<b>Years</b>
Cool	1900 – 1925
Warm	1926 – 1969
Cool	1970 – 1994
Warm	1995 - 2010

**Table 6: Temporal Windows for Positive and Negative Phases of NAO**

<b>Phase</b>	<b>Years</b>
Positive	1950 – 1951
Negative	1952 – 1972
Positive	1973 – 1976
Negative	1977 – 1980
Positive	1981 – 2001

## 5 RESULTS AND ANALYSIS

This chapter presents and provides interpretation of the results of this study. First, the results for the FDC analysis are discussed in section 5.1. FDC curves were created for the warm phase and the cool phase of each oscillation and the phase resulting in the lowest flows was determined. The FDC results were also mapped to determine spatial variability between the phases. In section 5.2 the results of the 7Q10 analysis are discussed. 7Q10 values were determined for the warm phase and the cool phase of each oscillation and the phase resulting in the lowest 7Q10 value was determined. The 7Q10 results were also mapped to determine spatial variability between phases. In section 5.3 the statistical significance testing of the 7Q10 values are discussed. In this section it was determined whether a statistically significant difference existed between the 7Q10 values for the warm and cool phases of each oscillation. In section 5.4, the temporal occurrences for the streamflow extremes are analyzed for the warm and cool phases of each oscillation. In section 5.5, the streamflow deficit analysis is discussed. Using the  $Q_{05}$  value as the streamflow deficit threshold value, the duration of deficit (days) for the warm phase and the cool phase of each oscillation is determined. A cumulative probability plot was created for the warm and cool phases for each station and the phase more likely to have greater than 30 days of deficit is determined. Finally, in section 5.6, the influences of AMO phases on spatial variability of streamflow extremes in Florida are examined.

## **5.1 Flow Duration Curves**

Flow duration curve analysis identifies intervals which can be used as a general indicator of hydrologic conditions. FDC intervals can be grouped into several broad categories: high flows (0 – 10%), moist conditions (10 – 40%), mid-range flows (40 – 60%), dry conditions (60 – 90%), and low flows (90 – 100%). Because the focus of this research is on low flows, special attention was paid to the low flow category with 90 – 100% exceedance frequency.

### **5.1.1 El Niño – Southern Oscillation**

For each FDC at every station, there are two curves: El Niño (red) and La Niña (blue). The shape of the FDC is determined by the hydrologic and geologic characteristics of the drainage area (Searcy, 1959). As such, the El Niño and La Niña curves tend to closely follow each other. Because low flows are of a concern, the region of 90 – 100% exceedance frequency is singled out of the graph. Each station is then categorized by which curve is “lower” than the other, that is, during low flow conditions, do El Niño or La Niña years have the smallest flows? The lowest flows for each station are outlined in Table 7. Stations marked with an (X) in the table indicate that the curves were nearly identical in the low flow section of the FDC. For these stations, there is no discernible difference between the low flows in El Niño and La Niña years and the results are inconclusive.

**Table 7: FDC-based Low Flow Occurrences for ENSO El Niño and La Niña Phases**

<b>Station Number</b>	<b>Lowest Flow Occurrence</b>
1	X
2	X
3	La Niña
4	X
5	X
6	El Niño
7	El Niño
8	X
9	El Niño
10	El Niño
11	El Niño
12	La Niña
13	La Niña
14	La Niña
15	La Niña
16	La Niña
17	El Niño
18	El Niño
19	La Niña
20	La Niña
21	El Niño
22	La Niña
23	El Niño
24	La Niña
25	X
26	La Niña
27	X
28	La Niña
29	La Niña
30	La Niña
31	El Niño
32	La Niña
33	La Niña
34	X
35	La Niña
36	La Niña
37	X
38	La Niña
39	La Niña
40	La Niña
41	La Niña
42	El Niño
43	El Niño

X: Inconclusive results

The majority of stations (53%) had lowest flows during the La Niña phase of ENSO. 28% of stations had lowest flows during El Niño phase and the remaining 19% of stations were inconclusive. To view the spatial variability of the FDC results, the stations are mapped in Figure 10. Black dots indicate that the results of the FDC curves were inconclusive, red dots indicate that El Niño years have lower flows, and blue dots indicate that La Niña years have lower flows.

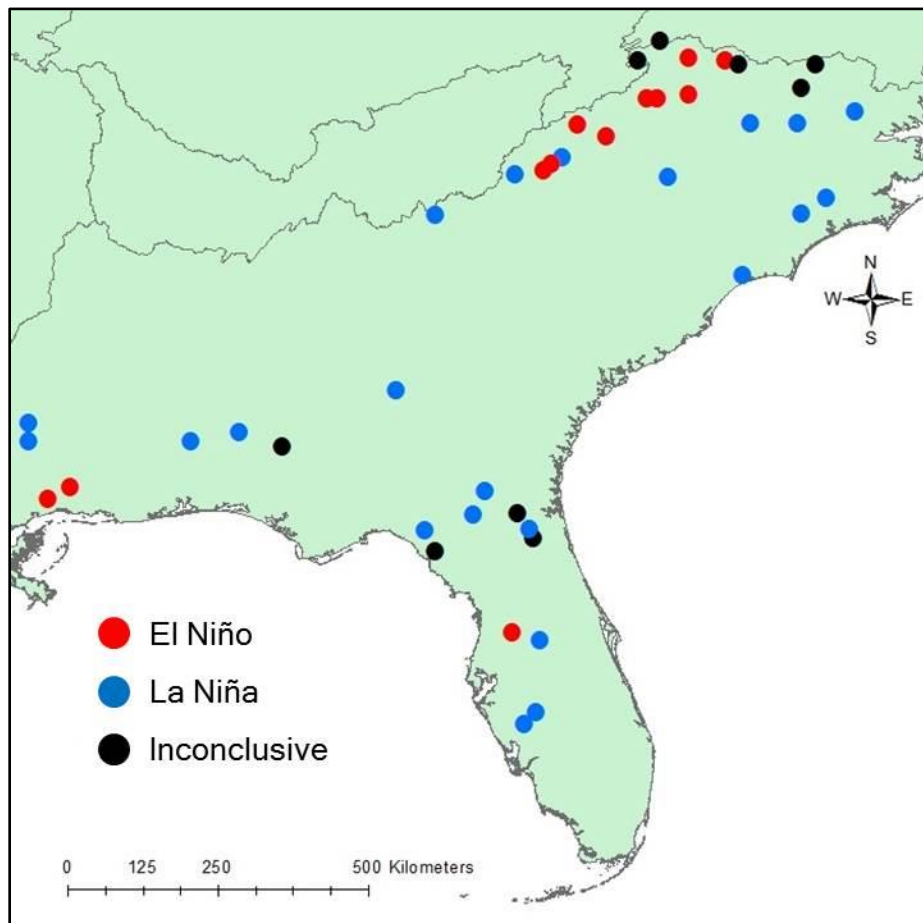


**Figure 10: Variability of FDC due to ENSO**

The data is then separated into 2 groups – north and south – for further analysis. The separated data is shown in Tables 8 and 9.

**Table 8: FDC-based Low Flow Occurrences for ENSO El Niño and La Niña Phases (Group 1)**

Station Number	Lowest Flow Occurrence
1	X
2	X
3	La Niña
4	X
5	X
6	El Niño
7	El Niño
8	X
9	El Niño
10	El Niño
11	El Niño
12	La Niña
13	La Niña
14	La Niña
15	La Niña
16	La Niña
17	El Niño
18	El Niño
19	La Niña
20	La Niña
21	El Niño
22	La Niña
23	El Niño
24	La Niña

X: Inconclusive results

**Table 9: FDC-based Low Flow Occurrences for ENSO El Niño and La Niña Phases (Group 2)**

Station Number	Lowest flow occurrence
25	X
26	La Niña
27	X
28	La Niña
29	La Niña
30	La Niña
31	El Niño
32	La Niña
33	La Niña
34	X
35	La Niña
36	La Niña
37	X
38	La Niña
39	La Niña
40	La Niña
41	La Niña
42	El Niño
43	El Niño

X: Inconclusive result

After the data is separated, the results in the northern section of the study domain were ambiguous. 21% of stations were inconclusive and the lowest flows occurred during El Niño years in 38% of the stations and La Niña years in 41% of the stations. 2 representative FDCs are shown in Figure 11: station 7 shows an example in which the El Niño FDC is lower than the La Niña, and station 19 shows an example when the La Niña FDC is lower than the El Niño.

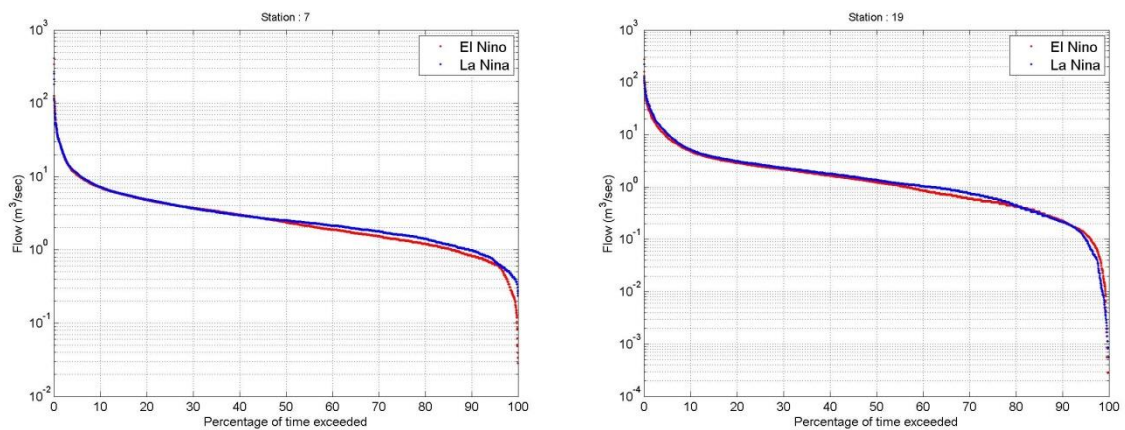


**Figure 11: FDCs of El Niño and La Niña Phases of ENSO at Select Stations**

**(Group 1)**

In the southern portion of the study domain, a specific pattern is more apparent. 63% of the stations experienced their lowest flows during La Niña years. Only 16% of stations had low flows during El Niño years and 11% of stations were inconclusive. 2 representative FDCs are shown in Figure 12. Both stations 35 and 39 show an example in which the La Niña FDC is lowest in the 90 – 100% exceeded range.



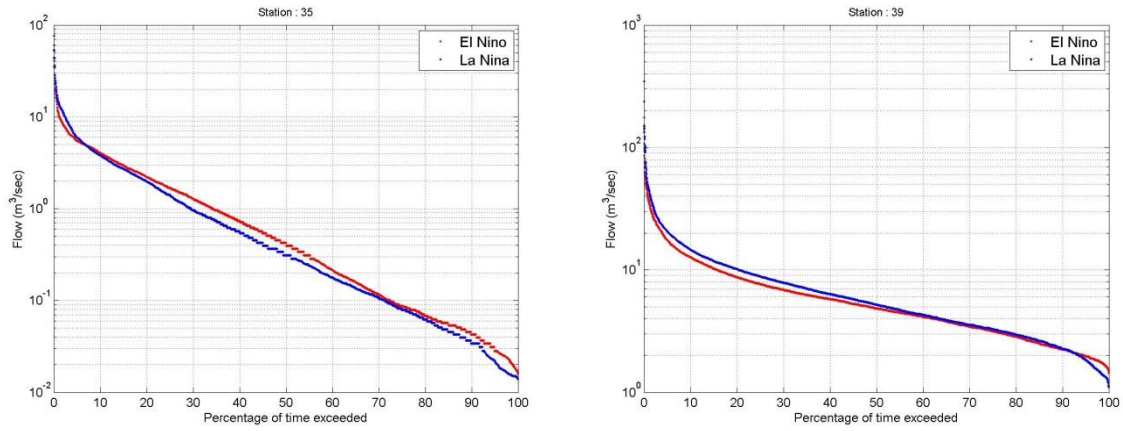


**Figure 12: FDCs of El Niño and La Niña Phases of ENSO at Select Stations**

**(Group 2)**

### 5.1.2 Pacific Decadal Oscillation

Table 10 outlines whether the lowest flows in the FDC occurred in the warm or cool phase of PDO.

**Table 10: FDC-based Low Flow Occurrences for PDO Warm and Cool Phases**

<b>Station Number</b>	<b>Lowest flow occurrence</b>
1	X
2	Cool
3	Cool
4	Cool
5	Cool
6	Cool
7	Cool
8	Cool
9	Cool
10	Cool
11	Cool
12	Cool
13	Cool
14	X
15	Cool
16	Cool
17	Cool
18	Cool
19	Cool
20	Cool
21	Cool
22	Cool
23	Cool
24	Cool
25	X
26	X
27	Cool
28	X
29	Cool
30	Cool
31	Cool
32	X
33	Warm
34	Cool
35	Cool
36	X
37	Cool
38	Cool
39	Cool
40	Cool
41	Cool
42	Cool
43	Cool

X: Inconclusive results

With only 2% of stations exhibiting low flows during the warm phase of PDO and 14% of stations that are inconclusive, the lowest flows mostly occurred in the cool phase of PDO (84% of all stations). A map of the FDC results is shown in Figure 13.

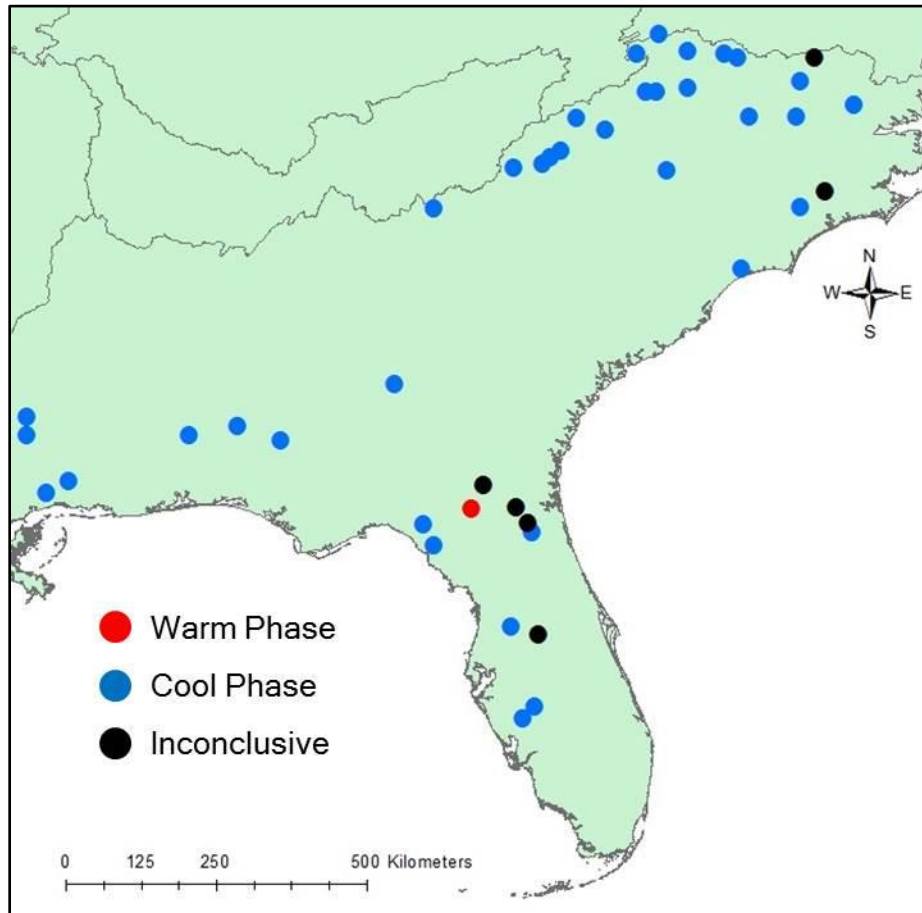


**Figure 13: Variability of FDC due to PDO**

The 4 sample FDCs of the both the north and south region (Figures 14 and 15, respectively) all show the lowest flows occurring during PDO cool phase years.

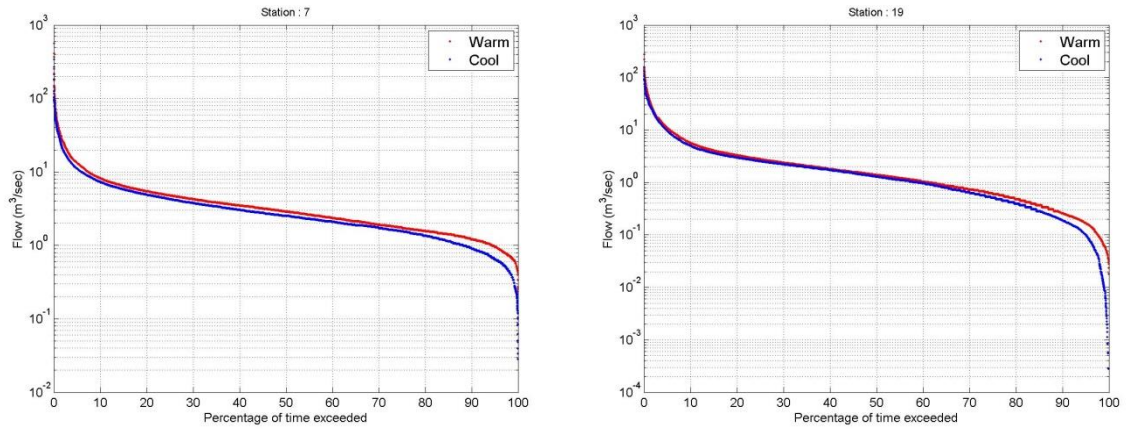


**Figure 14: FDCs of Warm and Cool Phases of PDO at Select Stations (Group 1)**

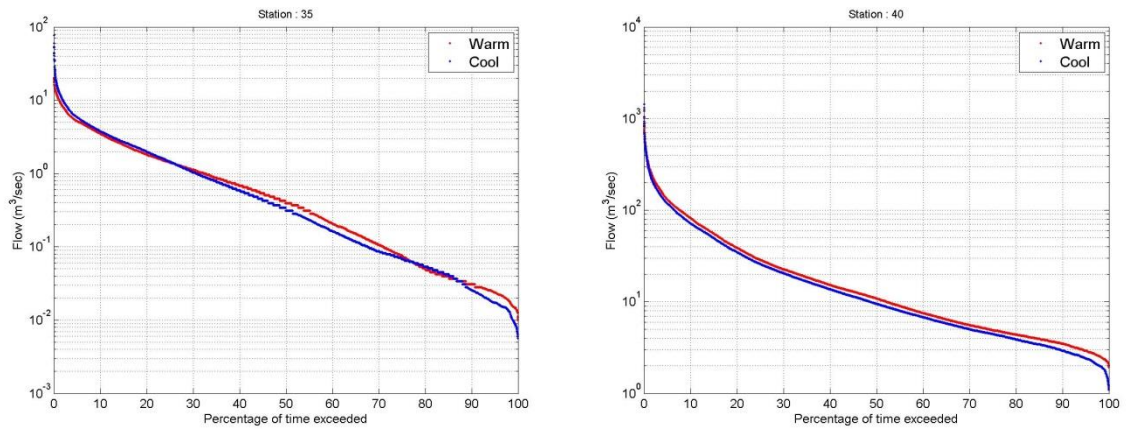


**Figure 15: FDCs of Warm and Cool Phases of PDO at Select Stations (Group 2)**

### 5.1.3 Atlantic Multidecadal Oscillation

Table 11 outlines whether the low flows in the FDC occur in the warm or cool phase of the AMO.

**Table 11: FDC-based Low Flow Occurrences for AMO Warm and Cool Phases**

<b>Station Number</b>	<b>Lowest Flow Occurrence</b>
1	X
2	Warm
3	Warm
4	Warm
5	Warm
6	Warm
7	Warm
8	Warm
9	Warm
10	Warm
11	Warm
12	Warm
13	Warm
14	X
15	Warm
16	Warm
17	Warm
18	Warm
19	Warm
20	Warm
21	Warm
22	Warm
23	Warm
24	Warm
25	Warm
26	Warm
27	Warm
28	Warm
29	Cool
30	Cool
31	Warm
32	Warm
33	Warm
34	Warm
35	Warm
36	X
37	X
38	X
39	Warm
40	Warm
41	Warm
42	Warm
43	Warm

X: Inconclusive results

From this table it is clear that the lowest flows for each station predominantly occur during the warm phase of the AMO. Only 4% of stations had low flows occurring during the cool phase of AMO and 12% of stations were inconclusive. The remaining 84% of stations all had experienced their lowest flows during warm phase years of the AMO. A map of the FDC results is shown in Figure 16.

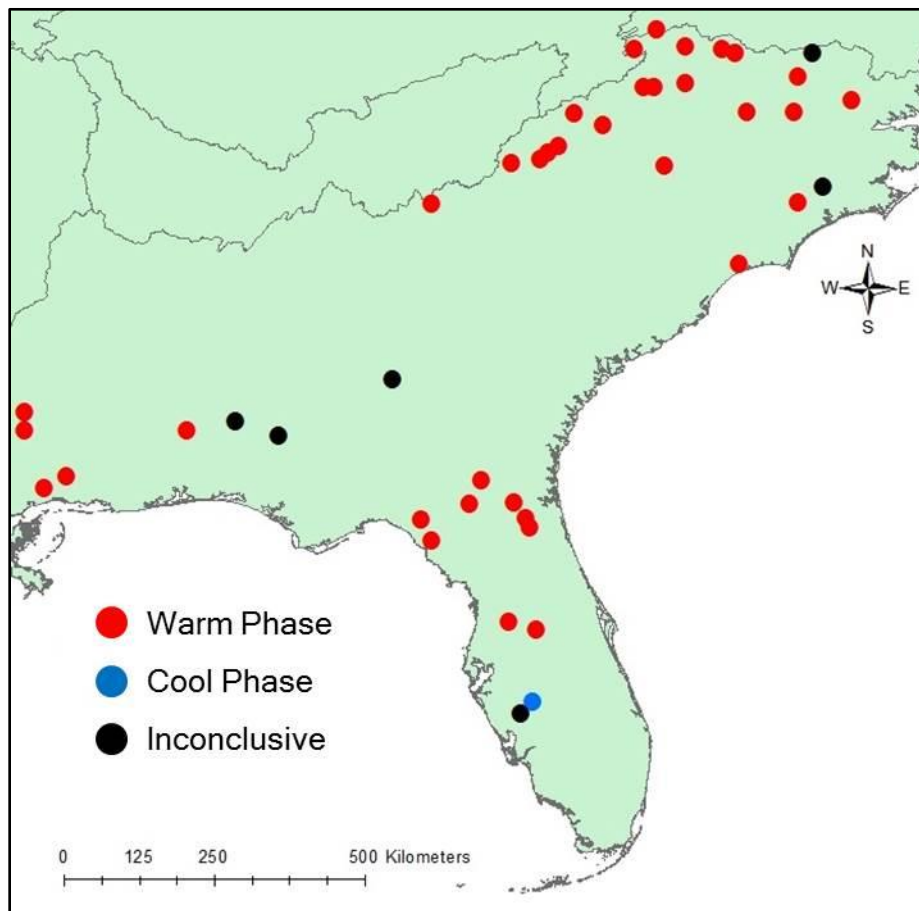


**Figure 16: Variability of FDC due to AMO**

The sample FDCs in Figures 17 and 18 all show lowest flows occurring during warm phase years of the AMO

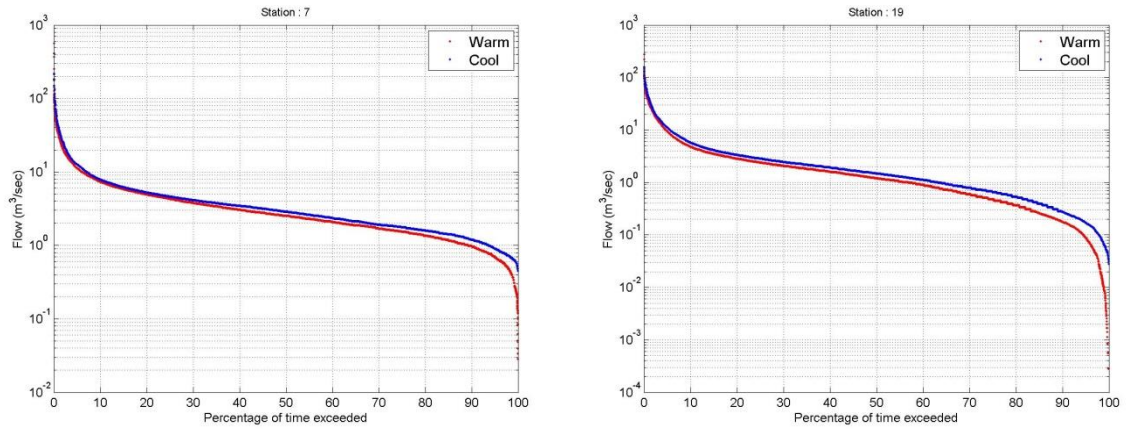


**Figure 17: FDCs of Warm and Cool Phases of AMO at Select Stations (Group 1)**

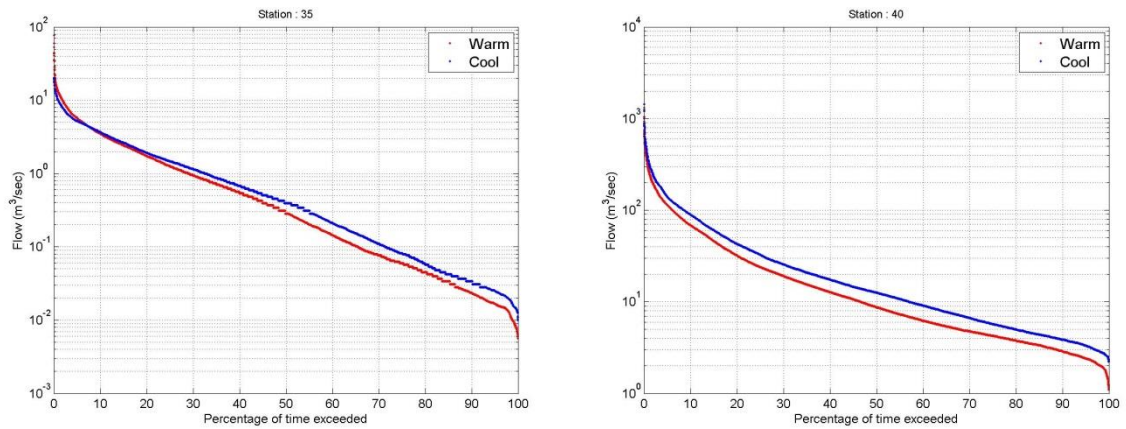


**Figure 18: FDCs of Warm and Cool Phases of AMO at Select Stations (Group 2)**

### 5.1.4 North Atlantic Oscillation

Table 12 shows whether the lowest flows in the NAO occur in either the positive or negative phase.

**Table 12: FDC-based Low Flow Occurrences for NAO Positive and Negative Phases**

<b>Station Number</b>	<b>Lowest Flow Occurrence</b>
1	Negative
2	Negative
3	X
4	Negative
5	X
6	X
7	Negative
8	Negative
9	X
10	Negative
11	Negative
12	Negative
13	Negative
14	Positive
15	Negative
16	Negative
17	X
18	X
19	Negative
20	Negative
21	Positive
22	X
23	Positive
24	X
25	Positive
26	Positive
27	Positive
28	Positive
29	Positive
30	X
31	Positive
32	Negative
33	X
34	Positive
35	Positive
36	Positive
37	Positive
38	Positive
39	Positive
40	Positive
41	X
42	Positive
43	Positive

X: Inconclusive Results



There is no obvious pattern for NAO. 42% of stations have their lowest flows during the positive phase of NAO, 33% of stations in the negative phase, and 25% of stations are inconclusive. A map of the FDC results is shown in Figure 19.

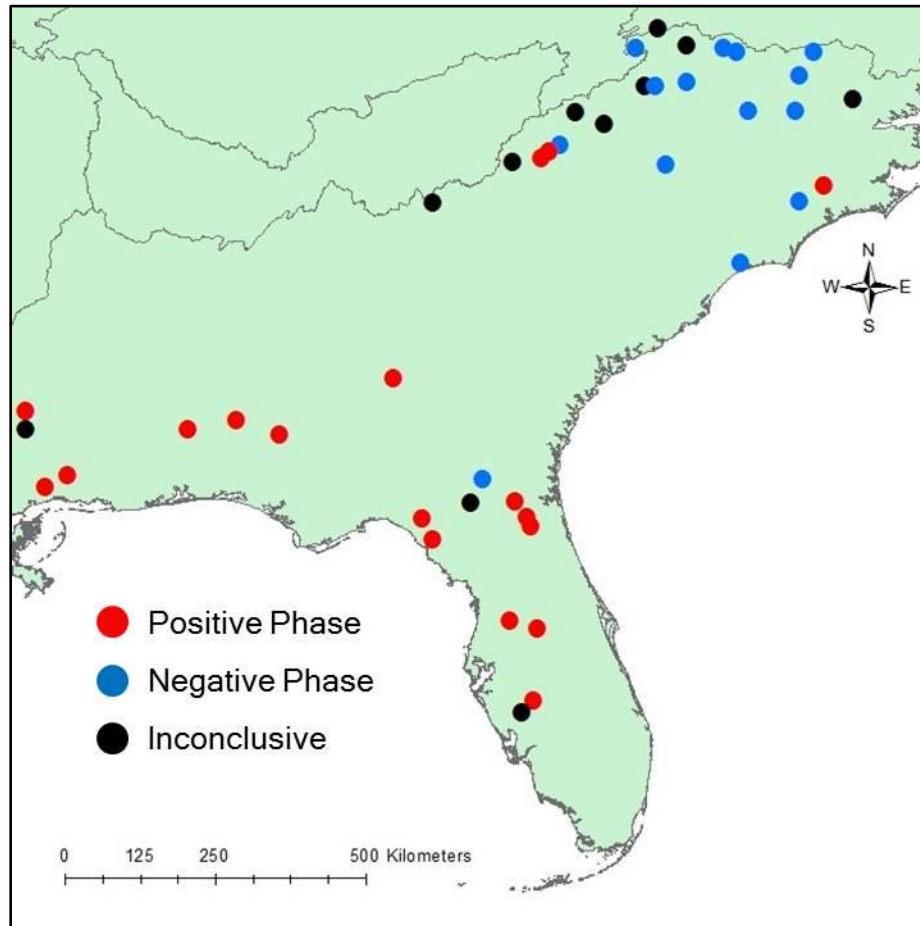


**Figure 19: Variability of FDC due to NAO**

However, if the stations are divided into 2 groups based on their geographic location (similar to the ENSO analysis), the NAO results are clearer. Table 13 includes stations 1 through 24, which is the northern portion of the study area, and Table 14 has the southern portion with stations 25 through 43.

**Table 13: FDC-based Low Flow Occurrences for NAO**

**Positive and Negative Phases (Group 1)**

Station Number	Lowest Flow Occurrence
1	Negative
2	Negative
3	X
4	Negative
5	X
6	X
7	Negative
8	Negative
9	X
10	Negative
11	Negative
12	Negative
13	Negative
14	Positive
15	Negative
16	Negative
17	X
18	X
19	Negative
20	Negative
21	Positive
22	X
23	Positive
24	X

X: Inconclusive results

**Table 14: FDC-based Low Flow Occurrences for NAO**

**Positive and Negative Phases (Group 2)**

Station Number	Lowest Flow Occurrence
25	Positive
26	Positive
27	Positive
28	Positive
29	Positive
30	X
31	Positive
32	Negative
33	X
34	Positive
35	Positive
36	Positive
37	Positive
38	Positive
39	Positive
40	Positive
41	X
42	Positive
43	Positive

X: Inconclusive results

For the NAO north region, only 13% of the stations had low flows occurring during the positive phase of NAO and 33% of stations were inconclusive. The remaining 54% stations all had their lowest flows during the negative phase of the NAO. In the sample FDCs shown in Figures 20, stations 7 and 19 in the northern region show low flows occurring during negative phase years of the NAO.

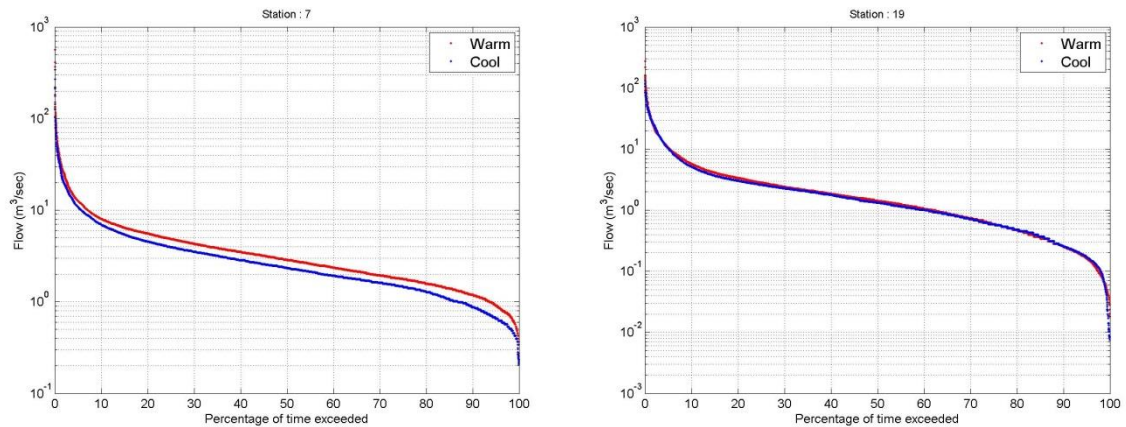


**Figure 20: FDCs of Positive and Negative Phases of NAO at Select Stations (Group 1)**

The opposite held true for the NAO south region. Only 5% of stations had lowest flows during the negative phase of NAO and 16% of stations were inconclusive. The majority of stations (79%) in the NAO south region had lowest flows during the NAO positive phase. Sample FDCs in Figure 21 show stations 35 and 40 in the southern region having low flows during the NAO positive phase years.

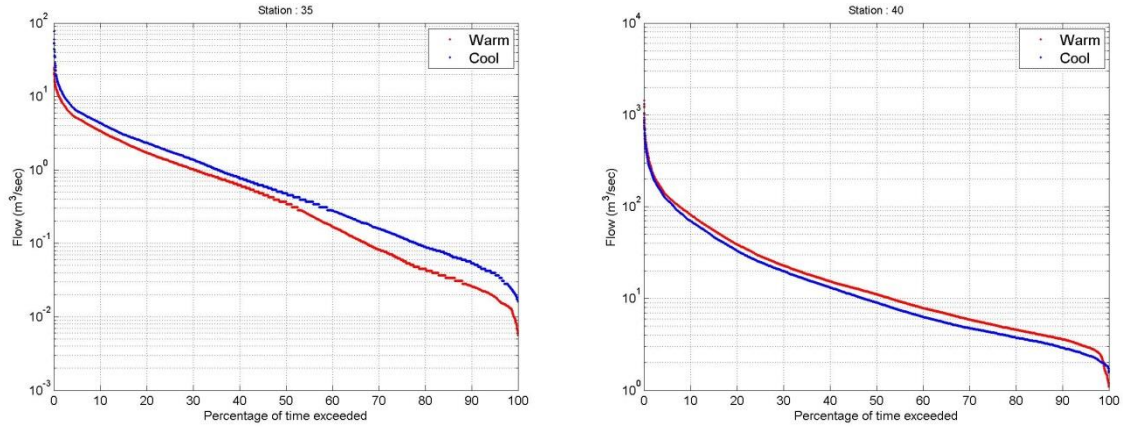


**Figure 21: FDCs of Positive and Negative Phases of NAO at Select Stations (Group 2)**

## 5.2 Low Flow Frequency Analysis

The 7Q10 values, i.e. the lowest 7-day average low flow that occurs on average once every 10 years, were computed for the warm and cool phase for each oscillation. The values between the warm and cool phase were compared and the phase which had the lowest 7Q10 was determined. Stations in which the difference between warm phase and cool phase 7Q10 values is less than  $0.10 \text{ m}^3/\text{s}$  are considered inconclusive and indicated with a (/).

### 5.2.1 El Niño – Southern Oscillation

Table 15 compares the 7Q10 values between the El Niño and La Niña phases of ENSO.

**Table 15: 7Q10 Values for ENSO El Niño and La Niña Phases**

Station Number	El Niño (m <sup>3</sup> /s)	La Niña (m <sup>3</sup> /s)	Lowest 7Q10 Occurrence
1	0.18	0.28	El Niño
2	10.39	12.38	El Niño
3	0.82	0.87	/
4	12.97	12.37	La Niña
5	0.78	0.88	El Niño
6	17.89	16.65	La Niña
7	7.23	11.01	El Niño
8	2.70	6.47	El Niño
9	20.83	22.80	El Niño
10	20.14	18.63	La Niña
11	11.11	12.24	El Niño
12	0.27	0.30	/
13	2.57	0.88	La Niña
14	1.29	0.70	La Niña
15	9.58	5.68	La Niña
16	10.86	7.56	La Niña
17	31.67	24.58	La Niña
18	26.27	22.01	La Niña
19	1.86	0.22	La Niña
20	13.67	12.54	La Niña
21	5.11	5.77	El Niño
22	25.84	17.75	La Niña
23	13.60	12.77	La Niña
24	114.05	83.65	La Niña
25	12.07	11.75	La Niña
26	0.05	0.06	/
27	9.92	10.35	El Niño
28	8.52	4.54	La Niña
29	0.99	0.37	La Niña
30	0.12	0.09	/
31	0.13	0.43	El Niño
32	2.89	1.31	La Niña
33	9.92	6.55	La Niña
34	4.09	3.22	La Niña
35	0.59	0.50	/
36	2.09	2.15	/
37	57.67	59.04	El Niño
38	21.21	20.79	La Niña
39	37.93	37.81	/
40	56.15	50.50	La Niña
41	87.87	77.19	La Niña
42	95.66	75.67	La Niña
43	2.37	1.63	La Niña

/: Inconclusive results

The majority of stations (58%) had the lowest 7Q10 values during La Niña years. 26% of stations had the lowest 7Q10 values during El Niño years and the remaining 26% of stations were inconclusive. A map of the ENSO 7Q10 results is shown in Figure 22.

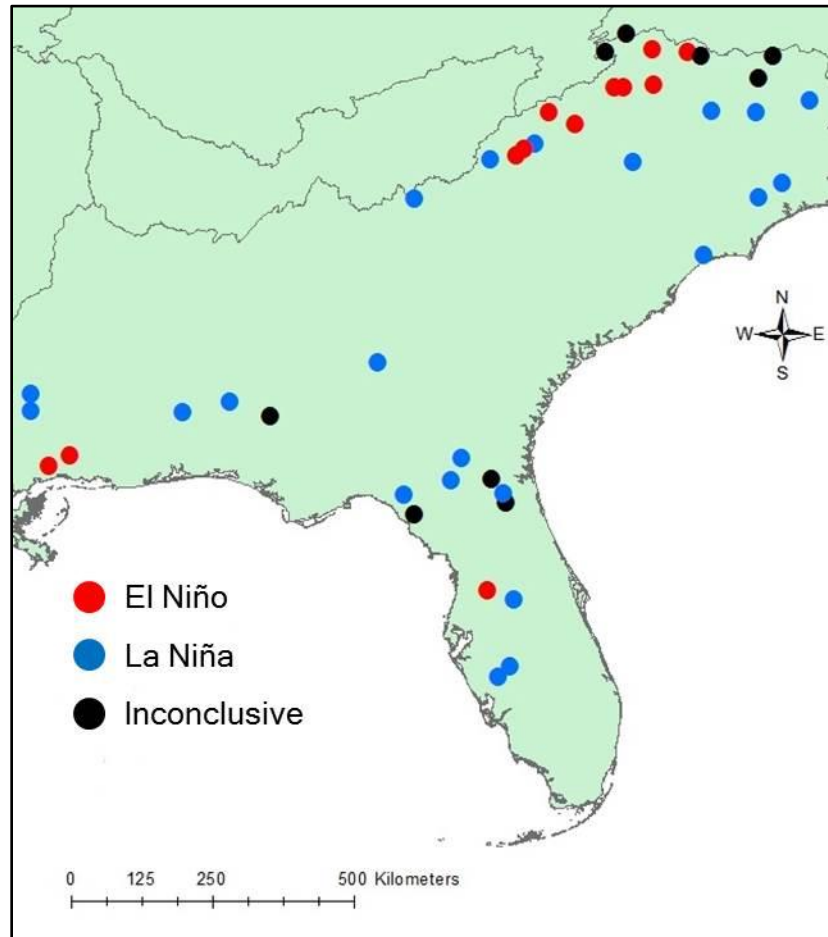


**Figure 22: Variability of 7Q10 due to ENSO**

### 5.2.2 Pacific Decadal Oscillation

Table 16 compares the 7Q10 values between the warm and cool phases of the PDO.

**Table 16: 7Q10 Values for PDO Warm and Cool Phases**

<b>Station Number</b>	<b>Warm Phase (m<sup>3</sup>/s)</b>	<b>Cool Phase (m<sup>3</sup>/s)</b>	<b>Lowest 7Q10 Occurrence</b>
1	0.19	0.25	/
2	14.72	11.45	Cool
3	0.57	0.45	Cool
4	14.52	10.42	Cool
5	1.07	0.79	Cool
6	20.20	16.78	Cool
7	17.64	9.51	Cool
8	12.71	4.69	Cool
9	27.71	20.80	Cool
10	28.31	20.08	Cool
11	X	12.05	X
12	0.16	0.19	/
13	1.69	1.47	Cool
14	0.89	0.99	Warm
15	8.51	8.41	Cool
16	9.95	5.47	Cool
17	38.58	27.71	Cool
18	33.30	27.19	Cool
19	0.99	0.34	Cool
20	21.27	13.49	Cool
21	6.89	5.07	Cool
22	29.89	21.25	Cool
23	18.68	13.05	Cool
24	112.87	102.63	Cool
25	9.85	13.66	Warm
26	0.01	0.01	/
27	11.98	9.61	Cool
28	4.88	5.46	Warm
29	0.65	0.42	Cool
30	0.34	0.09	Cool
31	0.07	0.45	Warm
32	2.46	3.95	Warm
33	4.77	13.02	Warm
34	3.09	X	X
35	0.35	0.29	/
36	2.21	2.32	Warm
37	66.34	57.21	Cool
38	X	19.76	X
39	61.20	X	X
40	73.16	54.59	Cool
41	108.81	80.63	Cool
42	116.90	74.10	Cool
43	2.53	X	X

/: Inconclusive results

X: Weibull distribution failed goodness-of-fit tests

For the PDO 7Q10 analysis, the data for 5 of the 43 stations could not be used because the Weibull distribution failed the goodness-of-fit tests at these stations. An additional 4 stations were considered inconclusive. A total of 21% of stations were therefore mapped as being “inconclusive.” The majority of stations (63%) had lowest 7Q10 values during the cool phase of AMO and only 16% during the warm phase. A map of the 7Q10 results is shown in Figure 23.

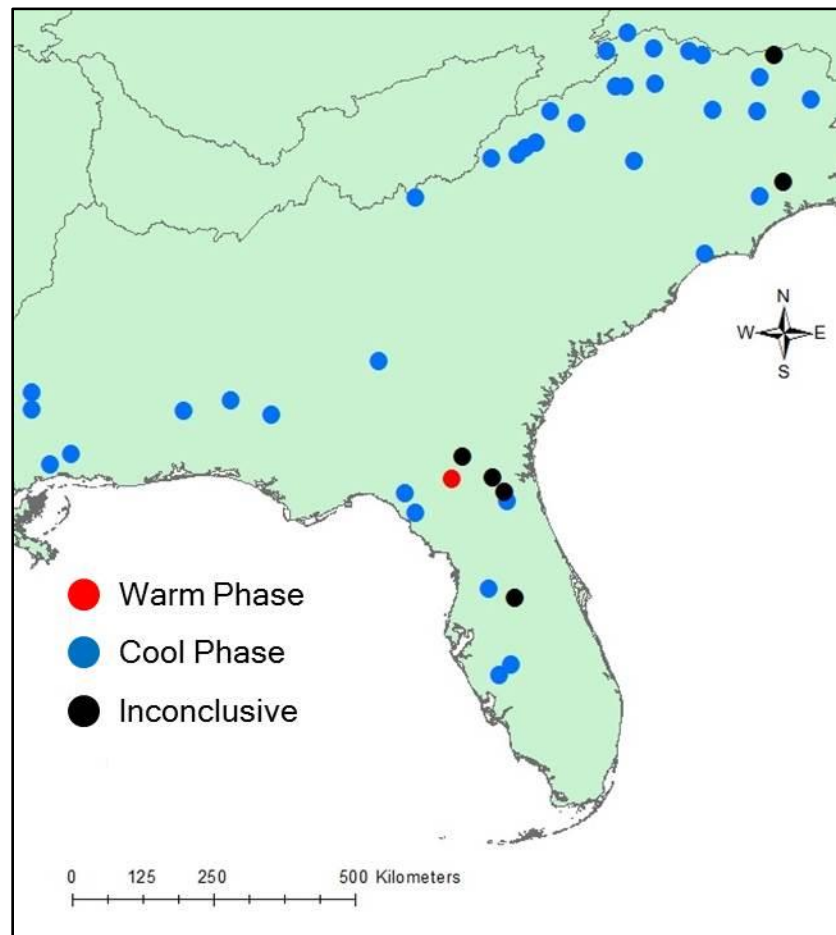


**Figure 23: Variability of 7Q10 due to PDO**

### 5.2.3 Atlantic Multidecadal Oscillation

Table 17 compares the 7Q10 values between the warm and cool phases of AMO.



**Table 17: 7Q10 Values for AMO Warm and Cool Phases**

Station Number	Warm Phase (m <sup>3</sup> /s)	Cool Phase (m <sup>3</sup> /s)	Lowest 7Q10 Occurrence
1	0.20	0.27	/
2	11.01	18.28	Warm
3	0.30	0.91	Warm
4	9.27	15.70	Warm
5	0.69	1.26	Warm
6	15.41	27.03	Warm
7	10.00	17.65	Warm
8	4.72	11.81	Warm
9	18.84	33.08	Warm
10	20.51	32.28	Warm
11	X	17.38	X
12	0.19	0.17	/
13	1.07	2.39	Warm
14	0.89	0.85	/
15	6.66	8.82	Warm
16	4.55	10.87	Warm
17	27.48	39.12	Warm
18	23.11	46.90	Warm
19	0.26	1.23	Warm
20	13.31	24.28	Warm
21	4.20	8.26	Warm
22	21.51	32.35	Warm
23	13.09	19.09	Warm
24	94.90	131.90	Warm
25	9.94	15.97	Warm
26	0.01	0.01	/
27	9.63	11.36	Warm
28	3.81	11.04	Warm
29	0.69	0.39	Cool
30	0.15	0.14	/
31	0.37	0.13	Cool
32	2.02	5.16	Warm
33	X	15.10	X
34	X	3.81	X
35	0.23	0.47	Warm
36	2.22	2.19	/
37	59.55	57.45	Cool
38	21.46	19.89	Cool
39	X	56.62	X
40	59.03	76.61	Warm
41	84.22	107.32	Warm
42	85.59	85.04	Cool
43	X	2.07	X

/: Inconclusive results

X: Weibull distribution failed goodness-of-fit tests

For the AMO, the data for 5 of the 43 stations could not be used because the Weibull distribution failed the goodness-of-fit tests at these stations. An additional 6 stations were considered inconclusive because the differences in 7Q10 values were less than  $0.10 \text{ m}^3/\text{s}$ . A total of 26% of stations were therefore mapped as “inconclusive.” The majority of stations (63%) had lowest 7Q10 values during the warm phase of AMO while only 11% of stations had lowest 7Q10 flows during the cool phase of AMO. A map of the 7Q10 results is shown in Figure 24.

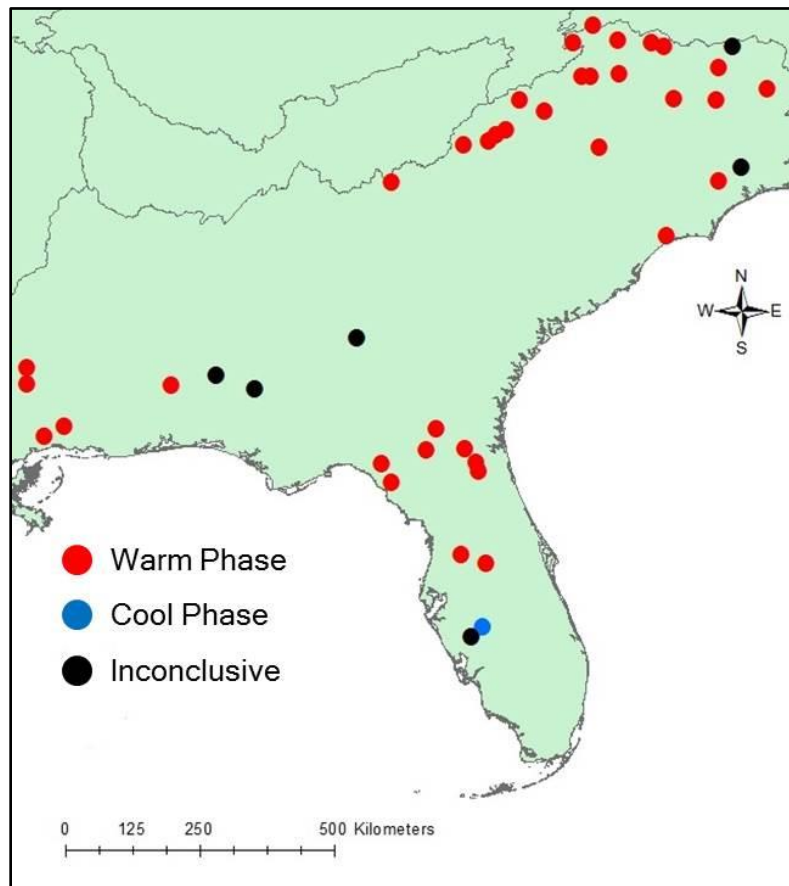


**Figure 24: Variability of 7Q10 due to AMO**

## 5.2.4 North Atlantic Oscillation

Table 18 compares the 7Q10 values between the warm and cool phases of the NAO.

**Table 18: 7Q10 Values for NAO Positive and Negative Phases**

Station Number	Positive Phase (m <sup>3</sup> /s)	Negative Phase (m <sup>3</sup> /s)	Lowest 7Q10 Occurrence
1	0.32	0.33	/
2	17.14	14.59	Negative
3	0.71	1.00	Positive
4	14.13	13.28	Negative
5	1.10	0.93	Negative
6	22.26	20.86	Negative
7	16.54	11.40	Negative
8	13.08	6.39	Negative
9	25.62	28.06	Positive
10	25.25	22.71	Negative
11	15.58	13.15	Negative
12	0.23	0.16	/
13	2.48	2.32	Negative
14	0.87	1.63	Positive
15	9.69	9.91	Positive
16	10.05	8.29	Negative
17	30.79	36.21	Positive
18	30.47	36.62	Positive
19	0.85	1.02	Positive
20	18.53	17.14	Negative
21	6.16	10.28	Positive
22	24.58	30.34	Positive
23	15.52	22.82	Positive
24	116.19	121.44	Positive
25	11.87	18.23	Positive
26	0.02	0.01	/
27	10.48	12.31	Positive
28	6.19	7.95	Positive
29	0.28	0.84	Positive
30	0.12	0.18	/
31	0.10	0.27	Positive
32	4.66	3.40	Negative
33	12.60	11.31	Negative
34	2.34	3.79	Positive
35	0.32	0.37	/
36	2.11	2.81	Positive
37	48.57	75.51	Positive
38	X	25.33	X
39	46.64	61.66	Positive
40	70.97	44.52	Negative
41	104.39	87.37	Negative
42	75.24	97.87	Positive
43	1.57	1.66	/

/: Inconclusive results

X: Weibull distribution failed goodness-of-fit tests

For the NAO 7Q10 analysis, 16% of stations were considered inconclusive. 1 station could not be used for failing the goodness-of-fit tests and 6 stations had differences between 7Q10 values that were less than  $0.10 \text{ m}^3/\text{s}$ . 49% of stations had lower 7Q10 flows during the positive phase of NAO while 35% had lower flows during the negative phase. A map of the 7Q10 results is shown in Figure 25. These results indicate that lowest 7Q10 values tend to occur during the positive phase of NAO; however, the data was divided into 2 groups for further analysis.

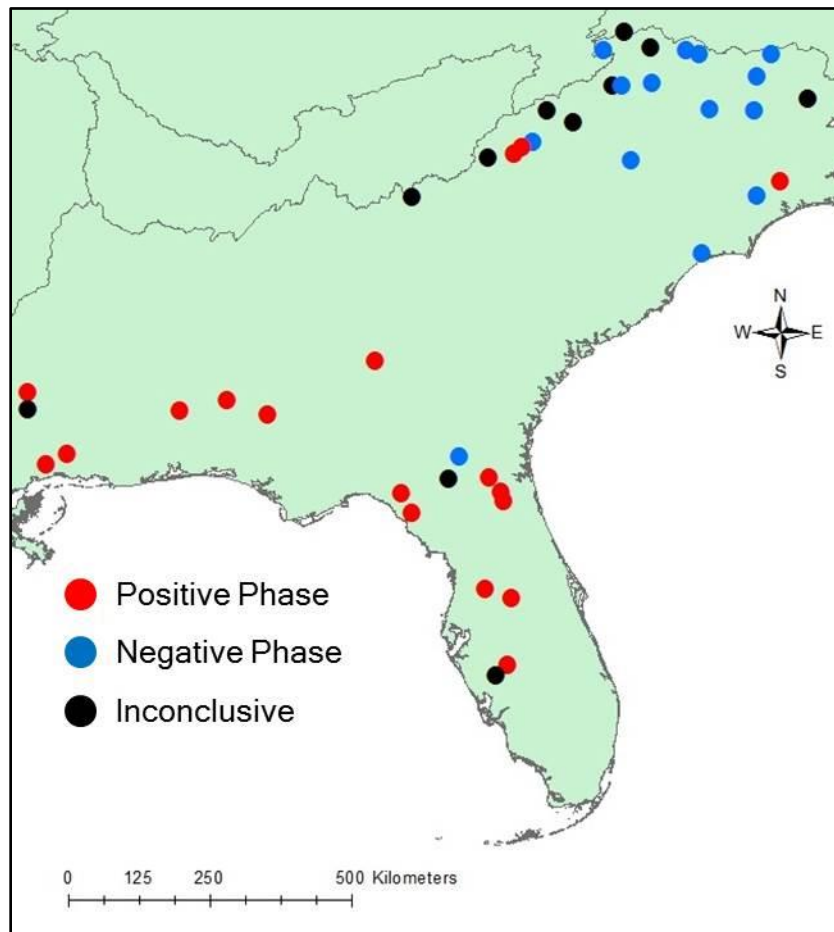


**Figure 25: Variability of 7Q10 due to NAO**

**Table 19: 7Q10 Values for NAO Positive and Negative Phases (Group 1)**

Station Number	Positive Phase (m <sup>3</sup> /s)	Negative Phase (m <sup>3</sup> /s)	Lowest 7Q10 Occurrence
1	0.32	0.33	/
2	17.14	14.59	Negative
3	0.71	1.00	Positive
4	14.13	13.28	Negative
5	1.10	0.93	Negative
6	22.26	20.86	Negative
7	16.54	11.40	Negative
8	13.08	6.39	Negative
9	25.62	28.06	Positive
10	25.25	22.71	Negative
11	15.58	13.15	Negative
12	0.23	0.16	/
13	2.48	2.32	Negative
14	0.87	1.63	Positive
15	9.69	9.91	Positive
16	10.05	8.29	Negative
17	30.79	36.21	Positive
18	30.47	36.62	Positive
19	0.85	1.02	Positive
20	18.53	17.14	Negative
21	6.16	10.28	Positive
22	24.58	30.34	Positive
23	15.52	22.82	Positive
24	116.19	121.44	Positive

/: Inconclusive results

**Table 20: 7Q10 Values for NAO Positive and Negative Phases (Group 2)**

Station Number	Positive Phase (m <sup>3</sup> /s)	Negative Phase (m <sup>3</sup> /s)	Lowest 7Q10 Occurrence
25	11.87	18.23	Positive
26	0.02	0.01	/
27	10.48	12.31	Positive
28	6.19	7.95	Positive
29	0.28	0.84	Positive
30	0.12	0.18	/
31	0.10	0.27	Positive
32	4.66	3.40	Negative
33	12.60	11.31	Negative
34	2.34	3.79	Positive
35	0.32	0.37	/
36	2.11	2.81	Positive
37	48.57	75.51	Positive
38	X	25.33	X
39	46.64	61.66	Positive
40	70.97	44.52	Negative
41	104.39	87.37	Negative
42	75.24	97.87	Positive
43	1.57	1.66	/

/: Inconclusive results

X: Weibull distribution failed goodness-of-fit tests

In group 1 (Table 19), the data remained ambiguous. 8% of stations were inconclusive, 46% of stations had lowest 7Q10 values during the positive phase of NAO, and 46% of stations had lowest 7Q10 values during negative phase of NAO. For group 2 (Table 20), the majority of stations (53%) had lowest 7Q10 values during the positive phase of NAO. 26% of stations were considered inconclusive and only 21% of stations had lowest 7Q10 values during the negative phase.

### **5.3 7Q10 Statistical Significance Analysis**

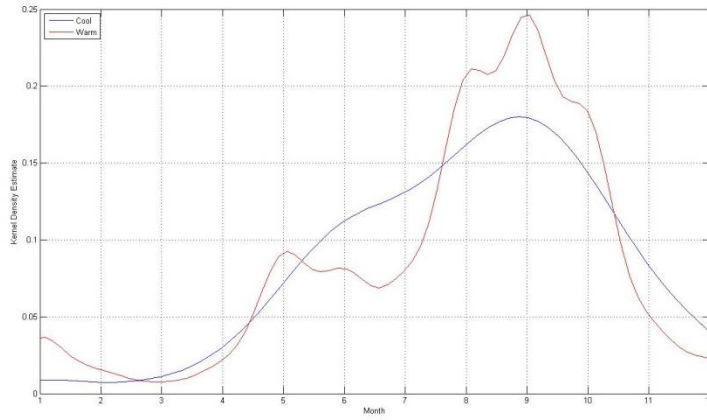
A two-sample unpaired t-test was performed on the 7Q10 values for the warm and cool phases of each oscillation. Initial results indicated that the null hypothesis ( $H_0$ ) was true for all oscillations, signaling that there is no significant difference between the 7Q10 values for warm and cool phases. To refine the analysis, 7Q10 values were divided geographically into 2 groups and the two-sample t-test was performed again. Again, the null hypothesis was true for groups 1 and 2 for all oscillations.

### **5.4 Temporal Variability Analysis**

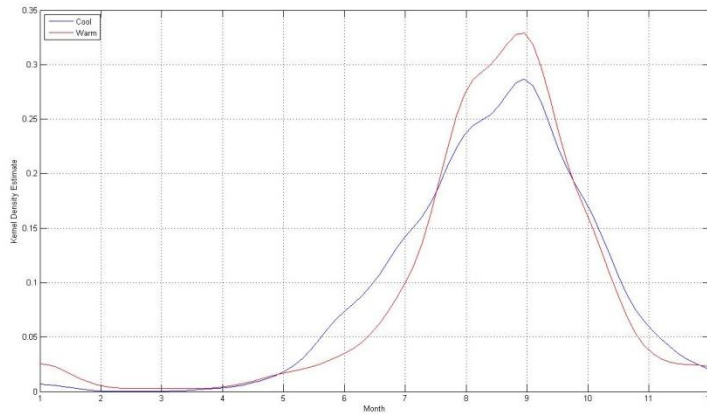
Kernel density estimates (KDE) were used to analyze the occurrence of AM7 values for the warm and cool phase of each oscillation. Initially, a single KDE graph was created for all 43 stations. To further refine the results, the stations were geographically divided into 2 groups and another KDE graph was created for each. The results for each oscillation are discussed below.

### 5.4.1 El Niño-Southern Oscillation

(a)



(b)



(c)

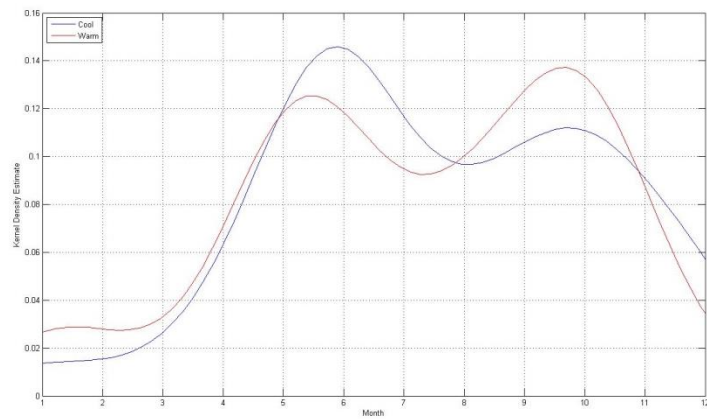


**Figure 26: Kernel Density Estimates of AM7 Occurrences for El Niño and La Niña**

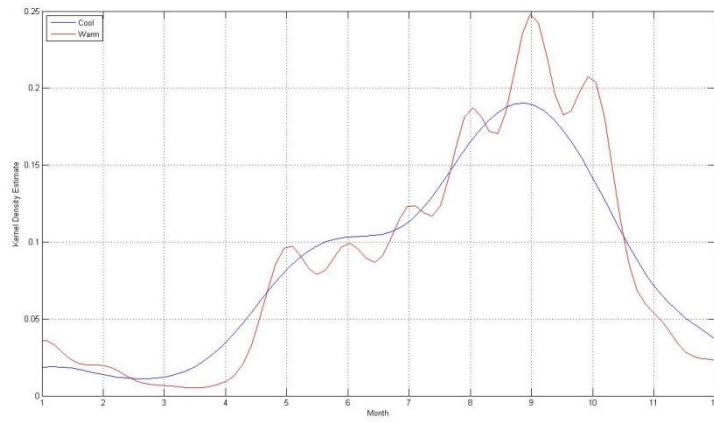
**Phases of ENSO (a) All Stations, (b) Group 1, (c) Group 2**

The KDE graph in Figure 26(a) is representative of all stations; however, this graph does not reveal much variation between El Niño and La Niña phases. The AM7 values tend to follow a general trend and both phases of ENSO have the most occurrences of low flows in September. The stations were then divided geographically for further analysis. Group 1, which is the northern group of stations (1 – 24), is shown in Figure 26(b). Group 2 is the southern group of stations (25 – 43) and is shown in Figure 26(c). For group 1, both El Niño and La Niña phases have the highest occurrence of AM7 during the late summer, peaking in the beginning of September. For group 2, there are 2 peak events: first in May/June, then in September. For the first low flow event in May, there are more AM7 occurrences during La Niña phase than El Niño phase. For the second low flow event in September, there are more AM7 occurrences during El Niño phase than La Niña phase.

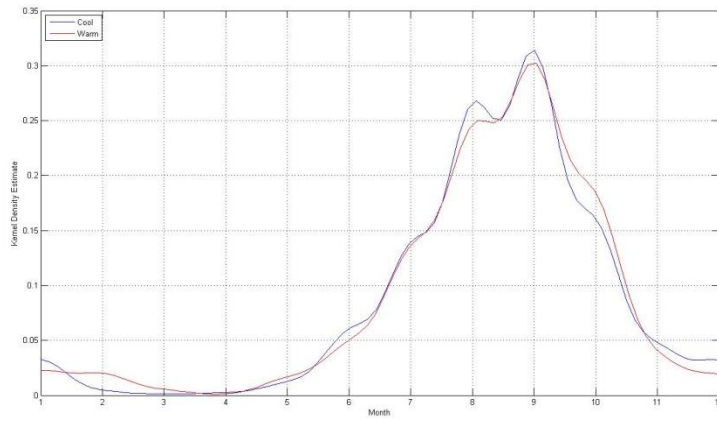


## 5.4.2 Pacific Decadal Oscillation

(a)



(b)



(c)

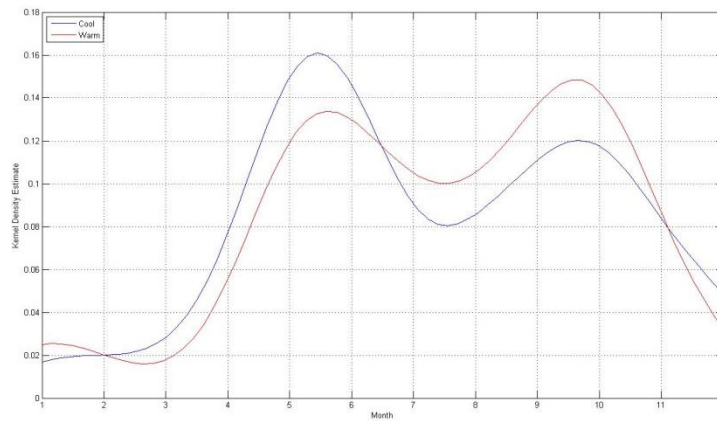


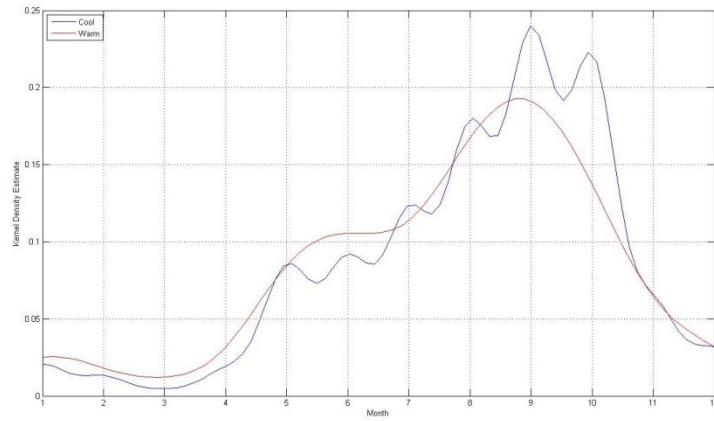
**Figure 27: Kernel Density Estimates of AM7 Occurrences for Warm and Cool**

**Phases of PDO (a) All Stations, (b) Group 1, (c) Group 2**

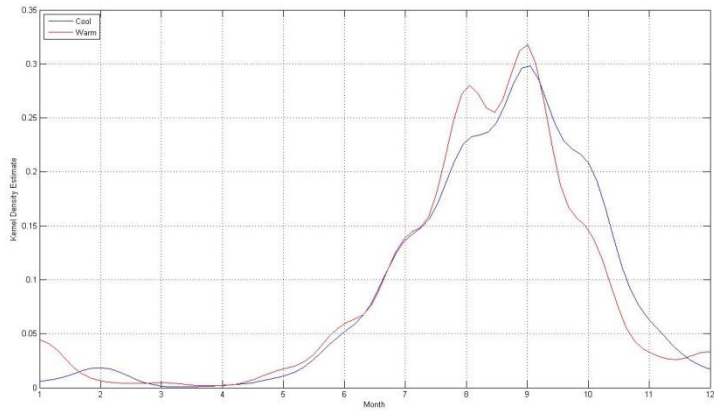
The KDE graph in Figure 27(a) is representative of all stations; however, this graph does not reveal much variation between warm and cool phases of PDO. The AM7 values tend to follow a general trend and both phases of PDO have the most occurrences of low flows in early September. The stations were divided geographically for further analysis. Group 1, which includes the northern group of stations (1 – 24), is shown in Figure 27(b). Group 2 is the southern group of stations (25 – 43) and is shown in Figure 27(c). For group 1, the occurrences of AM7 are very similar for both phases of PDO, peaking in the beginning of September. For group 2, there are 2 peak events: first in May, then in September. For the first low flow event in May, there are more AM7 occurrences during cool phase years than warm phase years of PDO. For the second low flow event in September, there are more AM7 occurrences during warm phase years than cool phase years of PDO.

### 5.4.3 Atlantic Multidecadal Oscillation

(a)



(b)



(c)

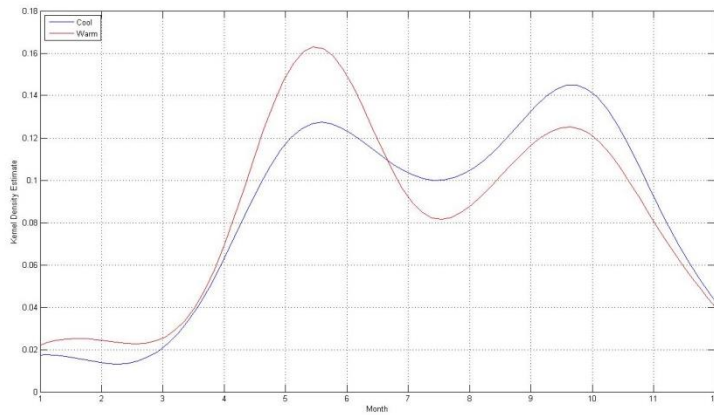


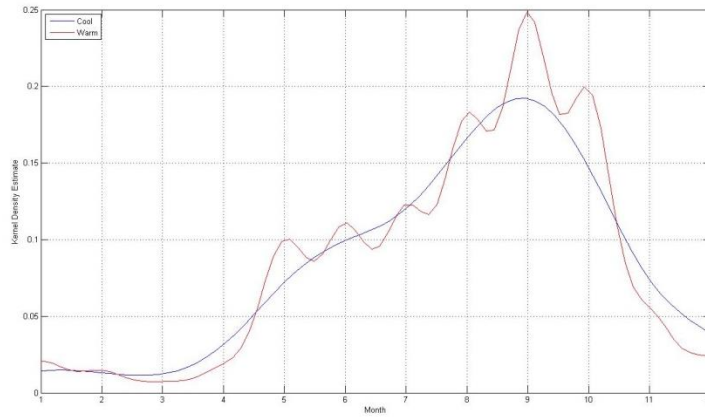
**Figure 28: Kernel Density Estimates of AM7 Occurrences for Warm and Cool**

**Phases of AMO (a) All Stations, (b) Group 1, (c) Group 2**

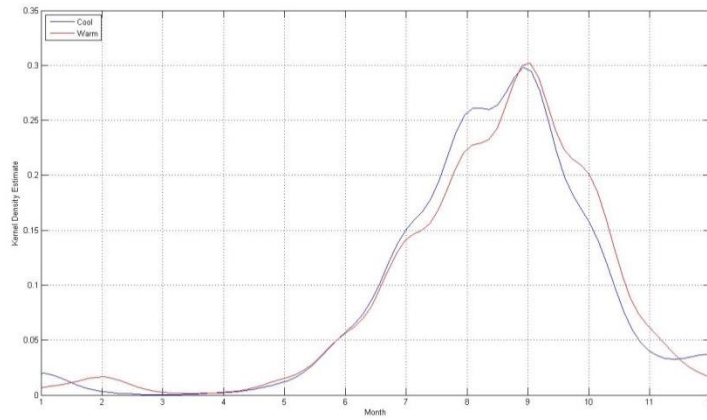
The KDE graph in Figure 28(a) is representative of all stations and shows that there are slight variations between the warm and cool phase of AMO. During the warm phase of AMO, the most occurrences of AM7 happen from mid-August through mid-September. However, during the cool phase of AMO, AM7 occurrences peak slightly later at the beginning of September and again at the beginning of October. The stations were divided geographically for further analysis. Group 1 includes stations 1 through 24 and is shown in Figure 28(b). Group 2 is stations 25 through 43 and is shown in Figure 28(c). For group 1, the most AM7 occurrences for both phases of AMO happen at the beginning of September. For group 2, there are 2 peak events: first in May and then in September. For the first low flow event in May, there are more AM7 occurrences during warm phase years of AMO than cool phase years. For the second low flow event in September, there are more AM7 occurrences during cool phase years of AMO than warm phase years.

## 5.4.4 North Atlantic Oscillation

(a)



(b)



(c)

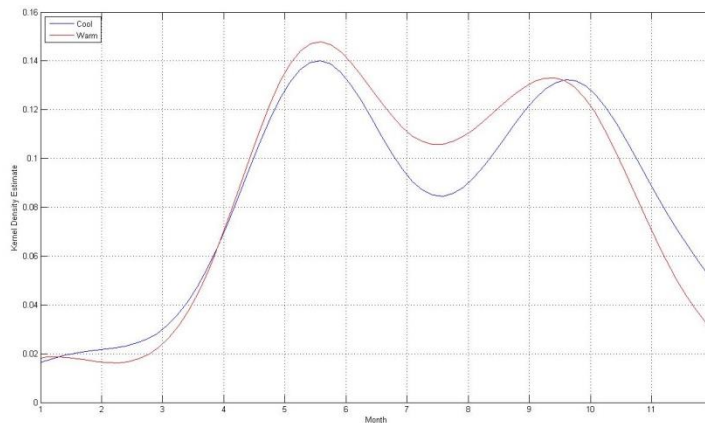


**Figure 29: Kernel Density Estimates of AM7 Occurrences for Positive and Negative Phases of NAO (a) All Stations, (b) Group 1, (c) Group 2**

The KDE graph in Figure 29(a) is representative of all stations; however, there is not much variation between the positive and negative phases of NAO. Both phases follow a general trend and AM7 values peak at the beginning of September. The stations are divided geographically into 2 groups for further analysis. Group 1 is the northern group of stations (1 – 24) and is shown in Figure 29(b). Group 2 is the southern group of stations (25 – 43) and is shown in Figure 29(c). For the first group of stations, peak AM7 occurrences happen at the beginning of September for both positive and negative phases of NAO. For the second group of stations, both phases of NAO closely follow each other and there are 2 peak occurrences of AM7 values: first during the month of May, and then again during the month of September.

## **5.5 Streamflow Deficit**

After the data had been divided into warm and cool phases, a streamflow deficit curve was created for each year in the period of record using the threshold value of  $Q_{95}$ . Once all of the deficit duration values were determined, a cumulative probability plot was created for the warm and cool phases for each station. Using the cumulative probability curve, it was determined which phase was “lower” at the 30 day mark, i.e., which phase was more likely to have greater than 30 days of deficit.

### **5.5.1 El Niño-Southern Oscillation**

Table 21 compares the probabilities that deficit durations will last longer than 30 days for El Niño and La Niña phases of ENSO. Stations marked with an (X) indicate that there is no discernible difference between phases at the 30 day mark and the results are inconclusive.

**Table 21: Streamflow Deficit Duration Analysis for El Niño and La Niña Phases of ENSO**

<b>Station Number</b>	<b>Greater Probability that Deficit Duration &gt; 30 days</b>
1	La Niña
2	La Niña
3	La Niña
4	La Niña
5	La Niña
6	X
7	X
8	X
9	El Niño
10	El Niño
11	El Niño
12	X
13	El Niño
14	El Niño
15	El Niño
16	El Niño
17	El Niño
18	El Niño
19	La Niña
20	El Niño
21	El Niño
22	El Niño
23	El Niño
24	X
25	El Niño
26	El Niño
27	El Niño
28	X
29	La Niña
30	X
31	X
32	X
33	El Niño
34	X
35	X
36	X
37	X
38	La Niña
39	X
40	El Niño
41	X
42	El Niño
43	El Niño

X: Inconclusive results

For the ENSO analysis, 35% of stations were considered inconclusive and 19% of stations had a greater probability of deficit durations greater than 30 days occur during La Niña years. However, the majority of stations (46%) had a greater probability of deficit durations greater than 30 days occurring during El Niño years. A map of the variability of deficit durations due to ENSO is shown in Figure 30.

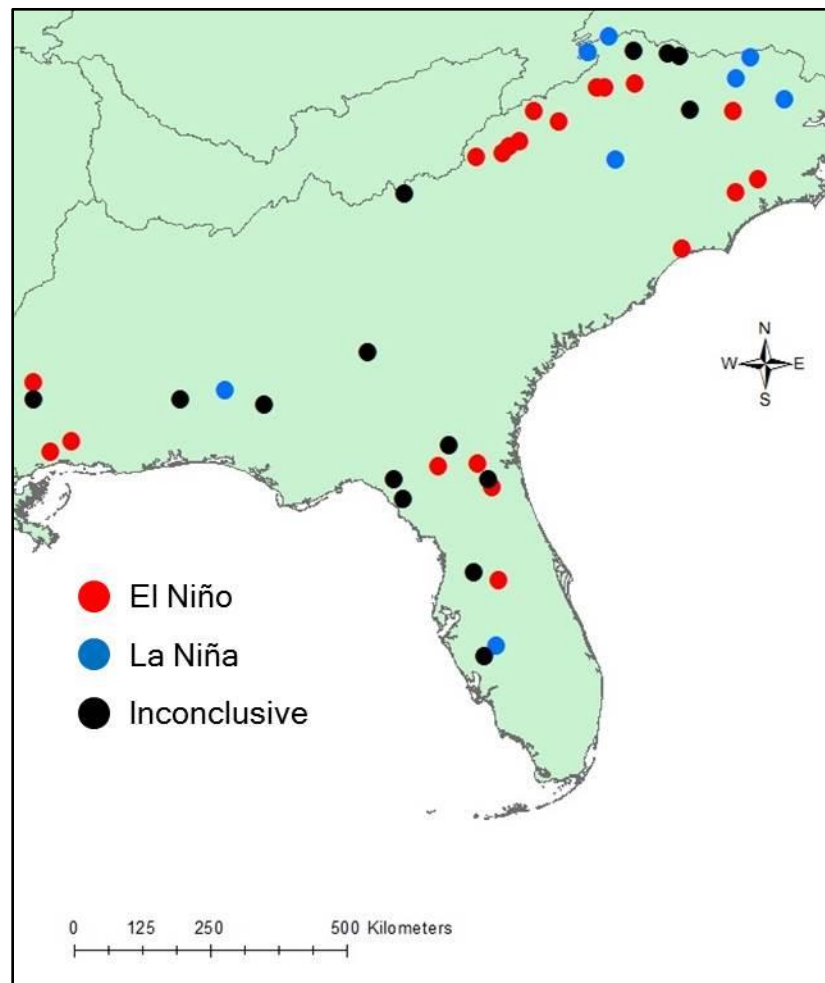


**Figure 30: Variability of Deficit Durations due to ENSO**

Select sample cumulative probability curves are shown in Figures 39 and 40. These samples all show that the greater probability of deficit durations lasting longer than 30 days occurred during the El Niño phase.



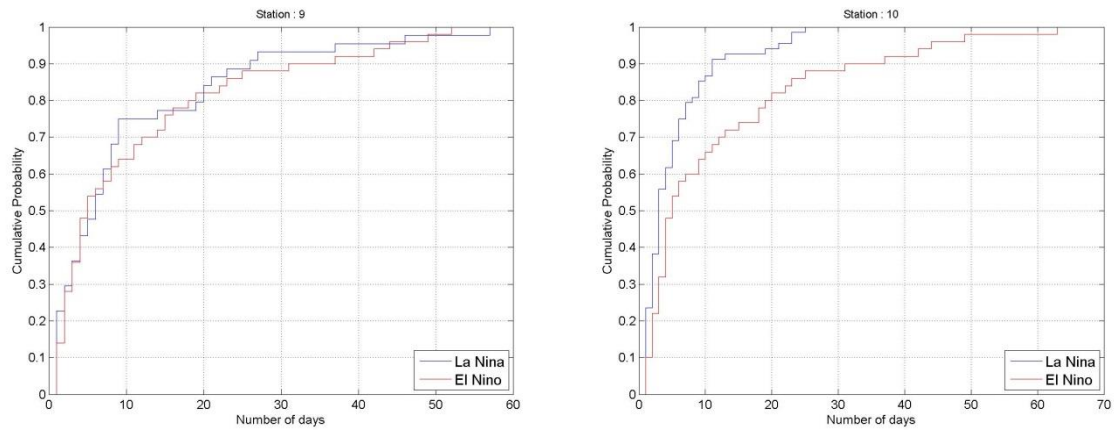


**Figure 31: Cumulative Probability Plots of Streamflow Deficit Duration for El Niño and La Niña Phases of ENSO at Select Stations (Group 1)**

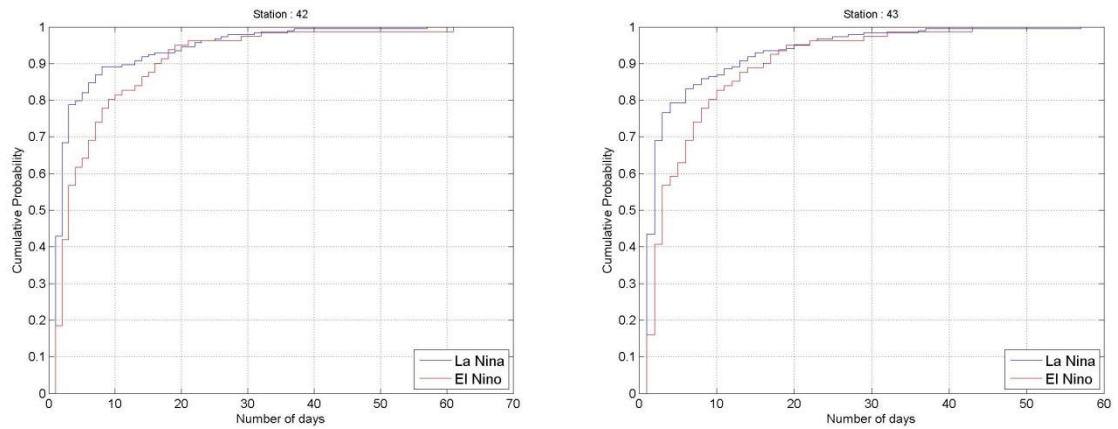


**Figure 32: Cumulative Probability Plots of Streamflow Deficit Duration for El Niño and La Niña Phases of ENSO at Select Stations (Group 2)**

### 5.5.2 Pacific Decadal Oscillation

Table 22 compares the probabilities that deficit durations will last longer than 30 days for warm and cool phases of PDO.

**Table 22: Streamflow Deficit Duration Analysis for Warm and Cool Phases of PDO**

<b>Station Number</b>	<b>Greater Probability that Deficit Duration &gt; 30 days</b>
1	Cool
2	Cool
3	Cool
4	X
5	Cool
6	Cool
7	Cool
8	Cool
9	Cool
10	Cool
11	X
12	Cool
13	Cool
14	X
15	X
16	Cool
17	Cool
18	Cool
19	Cool
20	X
21	Cool
22	Cool
23	Cool
24	Cool
25	X
26	X
27	Cool
28	X
29	Cool
30	Cool
31	Cool
32	Cool
33	X
34	X
35	Cool
36	Cool
37	Cool
38	Cool
39	X
40	Cool
41	Cool
42	Cool
43	Cool

X: Inconclusive results

For the PDO analysis, 74% of stations had a higher probability to have more than 30 days of deficit occur during the cool phase. The remaining 26% of stations were inconclusive and no stations had a higher probability for the warm phase of PDO. A map of the PDO results for deficit durations is shown in Figure 33.

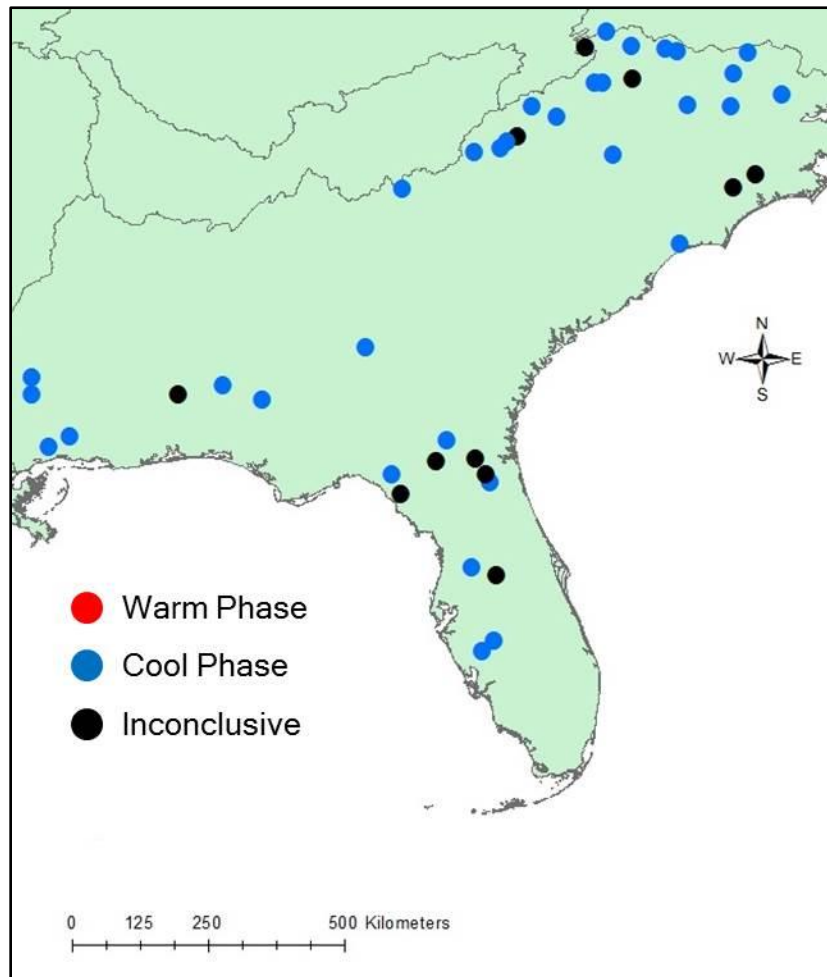


**Figure 33: Variability of Deficit Durations due to PDO**

Sample cumulative probability plots are shown in Figures 34 and 35. In all of these plots, there is a greater probability that deficit durations will last longer than 30 days for the cool phase of PDO.

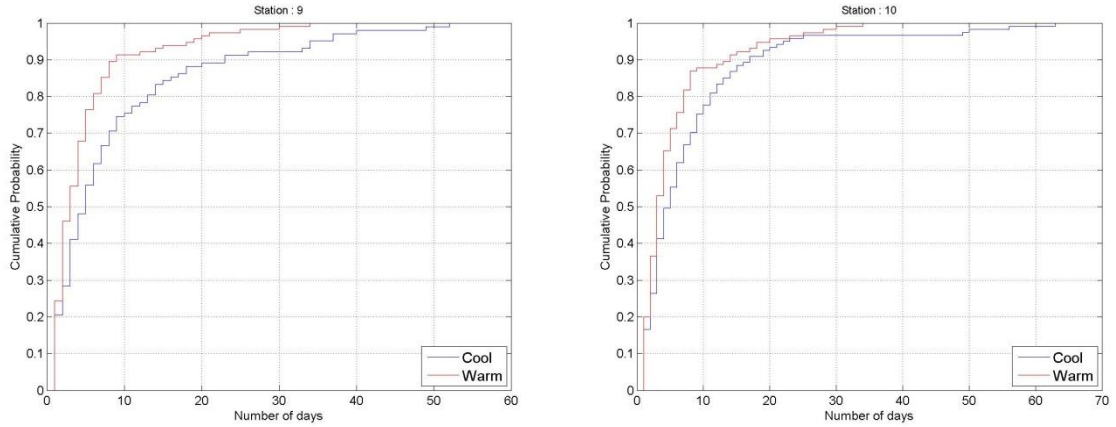


**Figure 34: Cumulative Probability Plots of Streamflow Deficit Duration for Warm and Cool Phases of PDO at Select Stations (Group 1)**

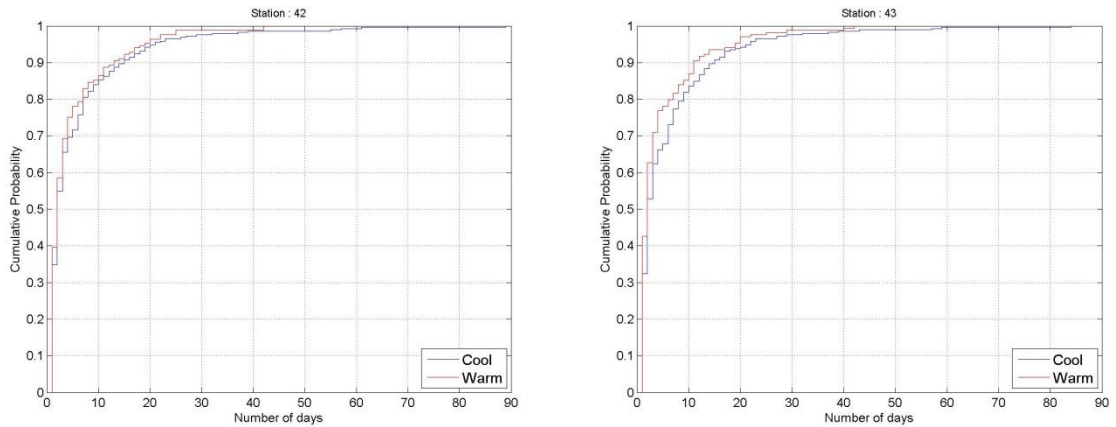


**Figure 35: Cumulative Probability Plots of Streamflow Deficit Duration for Warm and Cool Phases of PDO at Select Stations (Group 2)**

### 5.5.3 Atlantic Multidecadal Oscillation

Table 23 compares the probabilities that deficit durations will last longer than 30 days for warm and cool phases of AMO.

**Table 23: Streamflow Deficit Duration Analysis for Warm and Cool Phases of AMO**

Station Number	Greater Probability that Deficit Duration > 30 days
1	X
2	Warm
3	X
4	Cool
5	Warm
6	X
7	Warm
8	Warm
9	Warm
10	Warm
11	X
12	Warm
13	Cool
14	Cool
15	X
16	Warm
17	Warm
18	Warm
19	Warm
20	Warm
21	Warm
22	Warm
23	Warm
24	X
25	Warm
26	Warm
27	Warm
28	X
29	Cool
30	Cool
31	Cool
32	Cool
33	X
34	Cool
35	Cool
36	Warm
37	Cool
38	Cool
39	Cool
40	Cool
41	X
42	Cool
43	Cool

X: Inconclusive results

For the AMO, the results are almost evenly divided between the warm and cool phase. For 35% of stations, there is a greater probability that more than 30 days of deficit will occur during cool phase years. For 44% of stations, the greater probability occurs during warm phase years. The remaining 11% of stations were inconclusive. A map of the variability of deficit durations due to AMO is shown in Figure 36. The data is split into 2 groups based on their location for further analysis in Tables 24 and 25.

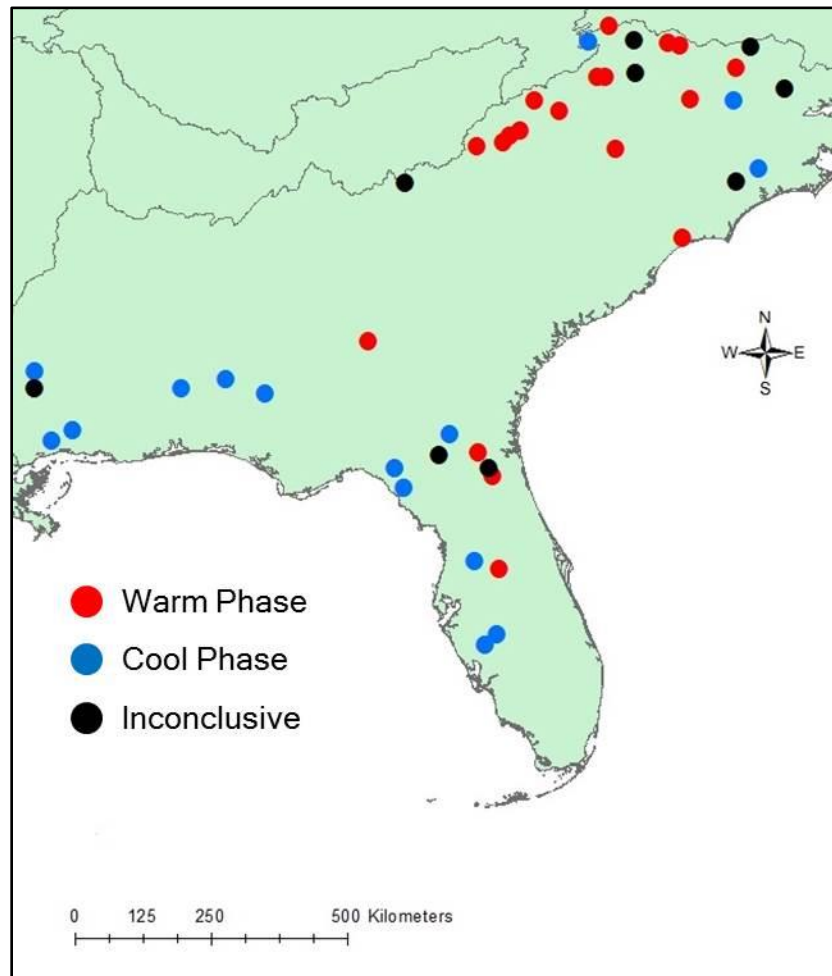


**Figure 36: Variability of Deficit Durations due to AMO**

**Table 24: Streamflow Deficit Duration Analysis for Warm and Cool Phases of AMO (Group 1)**

Station Number	Greater Probability that Deficit Duration > 30 days
1	X
2	Warm
3	X
4	Cool
5	Warm
6	X
7	Warm
8	Warm
9	Warm
10	Warm
11	X
12	Warm
13	Cool
14	Cool
15	X
16	Warm
17	Warm
18	Warm
19	Warm
20	Warm
21	Warm
22	Warm
23	Warm
24	X

X: Inconclusive results

**Table 25: Streamflow Deficit Duration Analysis for Warm and Cool Phases of AMO (Group 2)**

Station Number	Greater Probability that Deficit Duration > 30 days
25	Warm
26	Warm
27	Warm
28	X
29	Cool
30	Cool
31	Cool
32	Cool
33	X
34	Cool
35	Cool
36	Warm
37	Cool
38	Cool
39	Cool
40	Cool
41	X
42	Cool
43	Cool

X: Inconclusive results

For Group 1, which is the northern group of stations, 63% of stations have a greater possibility that deficit durations exceeding 30 days will occur during the warm phase of AMO. 12% of stations in this group had a greater possibility deficit duration exceeding 30 days occurring during the cool phase of AMO and 25% of stations were inconclusive. Sample cumulative probability curves are shown in Figure 37. For both plots there is a greater probability that deficit durations will last longer than 30 days for the warm phase of AMO.

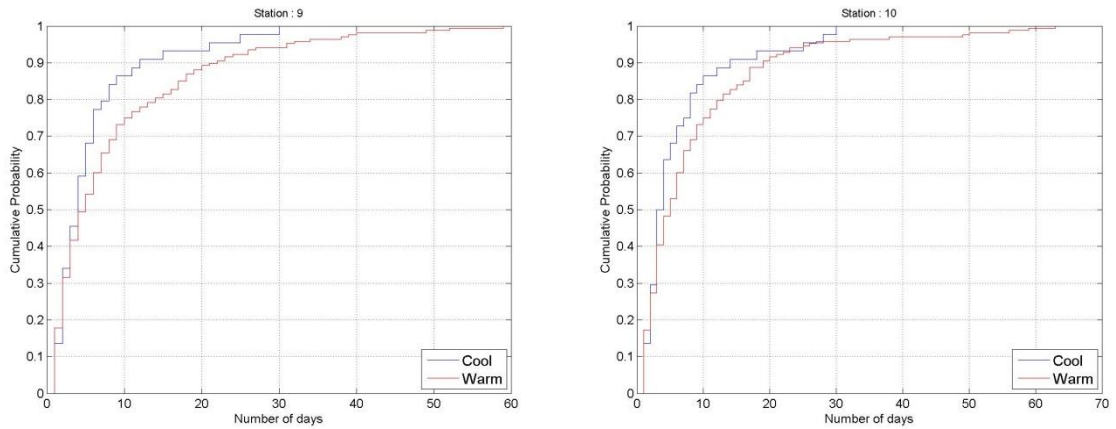


**Figure 37: Cumulative Probability Plots of Streamflow Deficit Duration for Warm and Cool Phases of AMO at Select Stations (Group 1)**

For Group 2, 63% of stations had a greater probability that a deficit duration that exceeds 30 days occurs during the cool phase of AMO. 21% of stations had a greater probability of longer deficits occurring during the warm phase and the remaining 16% were inconclusive. Sample cumulative probability curves are shown in Figure 38. For both plots there is a greater probability that deficit durations will last longer than 30 days for the cool phase of AMO.



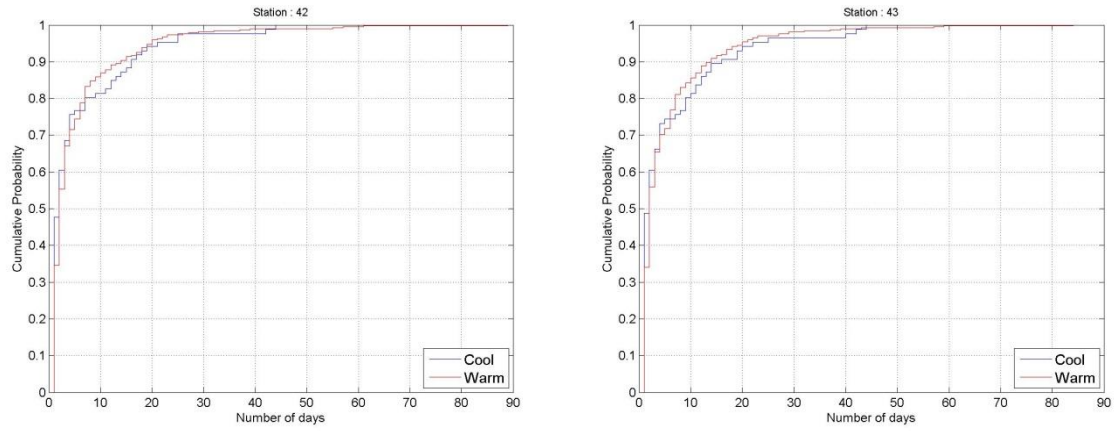


**Figure 38: Cumulative Probability Plots of Streamflow Deficit Duration for Warm and Cool Phases of AMO at Select Stations (Group 2)**

#### 5.5.4 North Atlantic Oscillation

Table 26 compares the probabilities that deficit durations will last longer than 30 days for positive and negative phases of NAO.

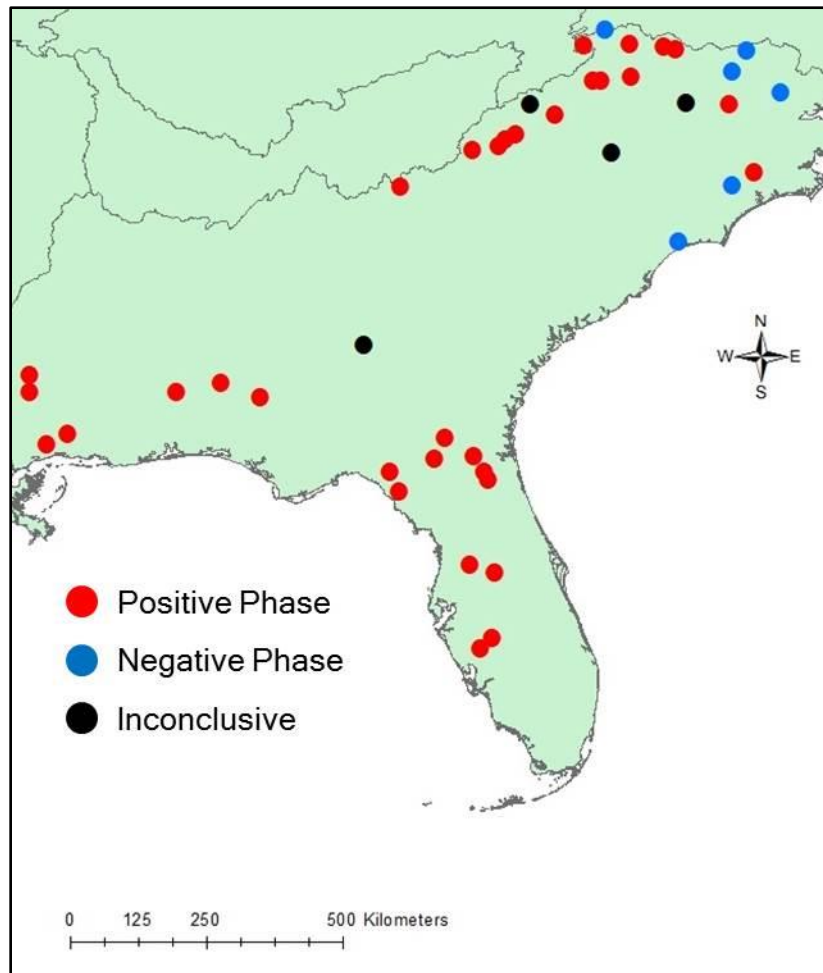
**Table 26: Streamflow Deficit Duration Analysis for Positive and Negative Phases of NAO**

<b>Station Number</b>	<b>Greater Probability that Deficit Duration &gt; 30 days</b>
1	Negative
2	Negative
3	Negative
4	Positive
5	Negative
6	Positive
7	Positive
8	Positive
9	Positive
10	Positive
11	Positive
12	X
13	Positive
14	Positive
15	Negative
16	Negative
17	X
18	Positive
19	X
20	Positive
21	Positive
22	Positive
23	Positive
24	Positive
25	Positive
26	Positive
27	Positive
28	Positive
29	Positive
30	Positive
31	Positive
32	Positive
33	Positive
34	Positive
35	Positive
36	X
37	Positive
38	Positive
39	Positive
40	Positive
41	Positive
42	Positive
43	Positive

X: Inconclusive results

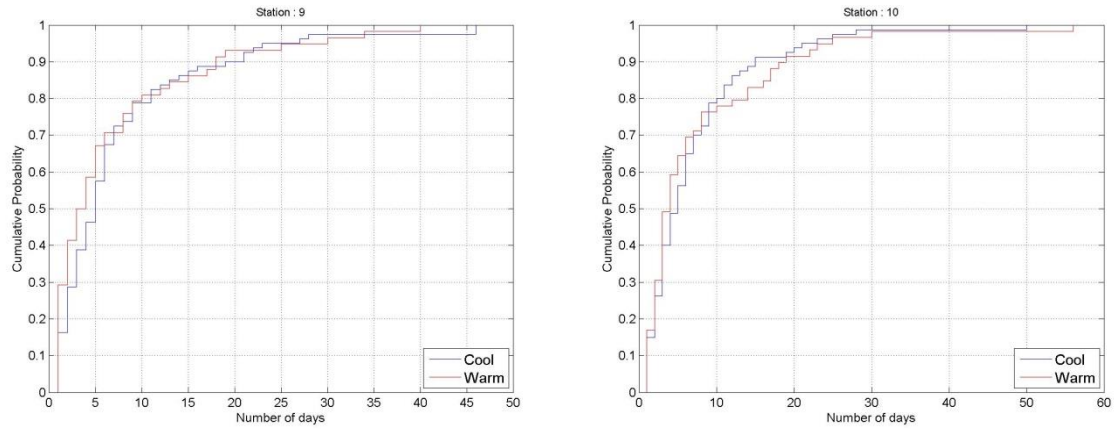
For NAO, the majority of stations (77%) had a greater probability of deficit durations lasting longer than 30 days occur during the positive phase. Only 14% of stations had a greater probability during the negative phase and 9% of stations were inconclusive.

Figure 39 shows a map of the deficit durations results.



**Figure 39: Variability of Deficit Durations due to NAO**

Figures 40 and 41 show the cumulative probability curves for NAO at select sites. For these stations, the probability for deficit durations lasting longer than 30 days is always greater during the positive phase of NAO.



**Figure 40: Cumulative Probability Plots of Streamflow Deficit Duration for Positive and Negative Phases of NAO at Select Stations (Group 1)**

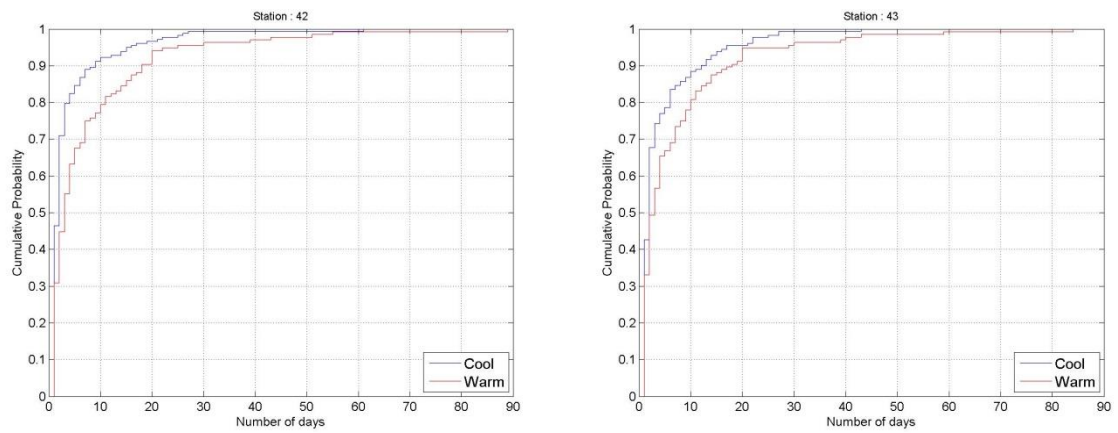


**Figure 41: Cumulative Probability Plots of Streamflow Deficit Duration for Positive and Negative Phases of NAO at Select Stations (Group 2)**

## 5.6 Influences of AMO Phases on Spatial Variability of Streamflow Extremes in Florida

According to Goly and Teegavarapu, the state of Florida can be approximately divided into two regions with: (1) peninsular climate in the south and (2) continental climate in the north (2014). Spatially varying statistical hypothesis tests indicate that

positive significance occurs in the peninsular south while negative significance occurs in the continental north. That is, there is increased rain during the warm phase of AMO in the southern region and increased rain during the cool phase of AMO in the northern region. It would be reasonable to assume that streamflow follows a similar pattern and that low flows would occur in the opposite phase of high rainfall. For the northern continental region, low flows should occur during the warm phase of AMO and for the southern peninsular region, low flows should occur during the cool phase of AMO.

There are 10 stations located in Florida. Stations 26, 29, 30, and 31 are in the southern peninsular region. Stations 25, 27, 28, 33, 34, and 35 are in the northern continental region. Section 5.6.1 will analyze the FDCs, 7Q10 values, and deficit durations for the southern peninsula region while section 5.6.2 will analyze these same indices for the northern continental region.

### **5.6.1 Florida Southern Peninsular Region**

The FDCs for the 4 stations in the southern peninsular region of Florida are shown in Figure 42. For this region we expect to see the smaller flows in the low flow region occur during the cool phase of AMO. This assumption was true for only 2 out of the 4 stations; however, these 2 stations were the only stations in the whole study domain to exhibit low flows during the AMO cool phase.

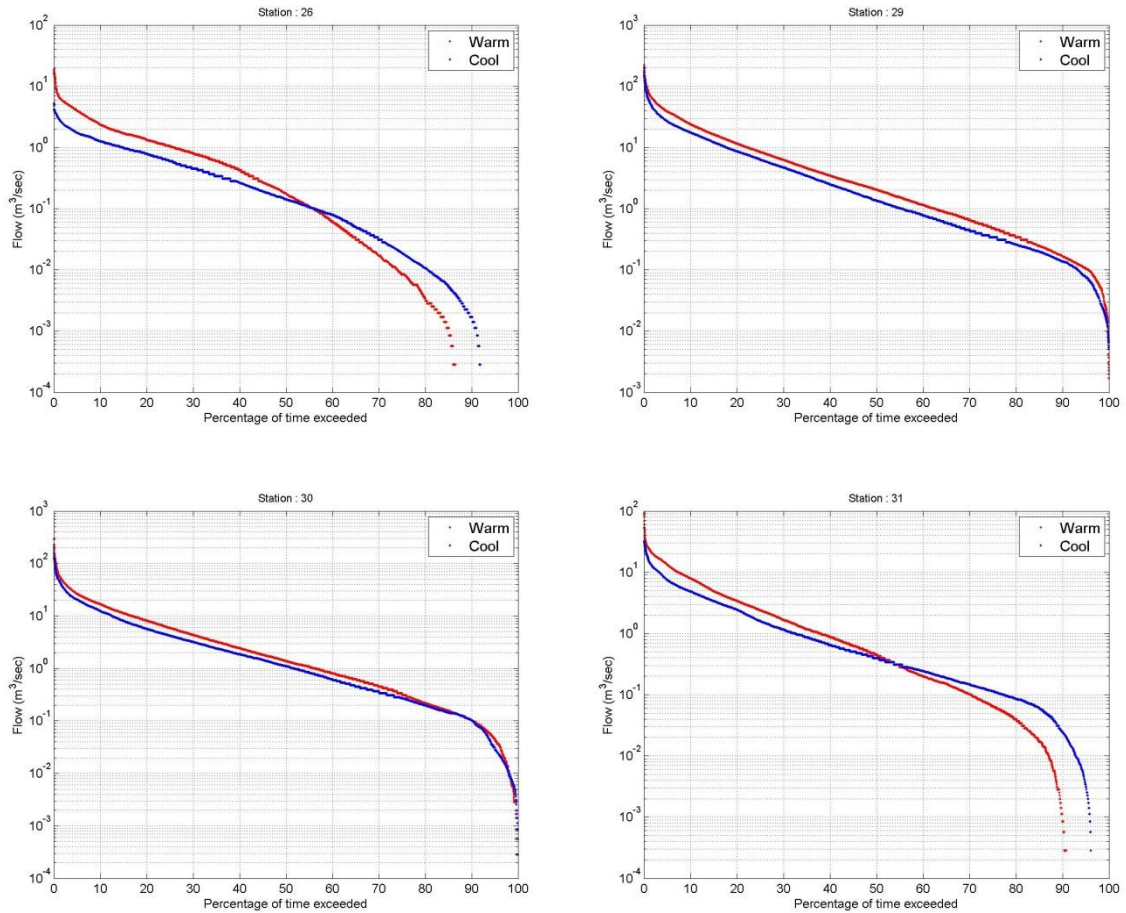


**Figure 42: FDCs of Warm and Cool Phases of AMO (Florida Southern Peninsular Region)**

Table 27 shows the 7Q10 values for the 4 stations in the southern peninsular region. Again, we expect to see the lowest flows occur during the cool phase of AMO. For this index, 3 out of 4 stations had their lowest 7Q10 value occur during the cool phase of AMO. Station 26 is considered inconclusive because the difference in 7Q10 values between warm and cool phases is less than 0.10 m<sup>3</sup>/s.

**Table 27: 7Q10 Values for AMO Warm and Cool Phases (Florida Southern Peninsula Region)**

Station Number	Warm Phase (m <sup>3</sup> /s)	Cool Phase (m <sup>3</sup> /s)	Lowest 7Q10 Occurrence
26	0.01	0.01	/
29	0.69	0.39	Cool
30	0.15	0.14	Cool
31	0.37	0.13	Cool

/: Inconclusive results

Figure 43 shows the cumulative probability streamflow deficit duration curves. For this region, we expect to see that cool phase is more likely to have greater than 30 days of deficit. The results show that 3 out of 4 stations exhibit this anticipated behavior.

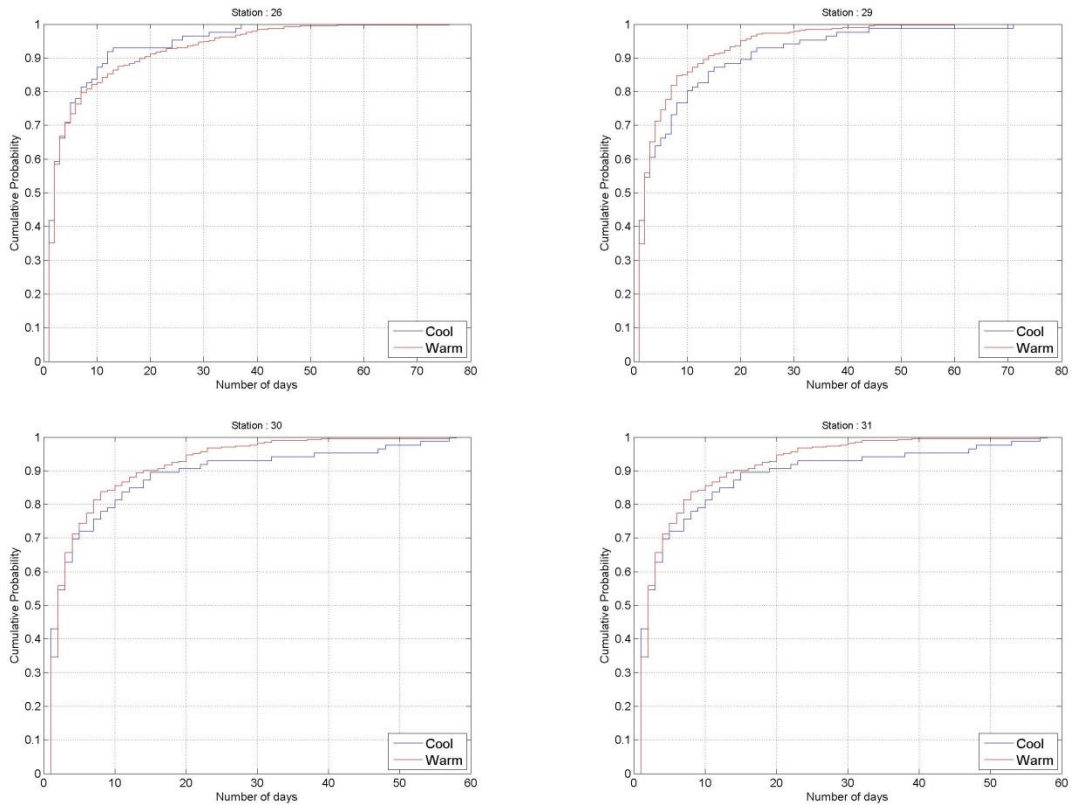


**Figure 43: Cumulative Probability Plots of Streamflow Deficit Duration for Warm and Cool Phases of AMO (Florida Southern Peninsular Region)**

For the southern peninsular region, the expected pattern of low flow occurring during the cool phase of AMO held up for all 3 indices.

### **5.6.2 Florida Northern Continental Region**

For Florida's northern continental region, we anticipate that all low flow indices predominantly occur during the warm phase of AMO. The FDCs for the 6 stations in this region are shown in Figure 44. As expected, all 6 stations had lower flows during the warm phase of AMO.



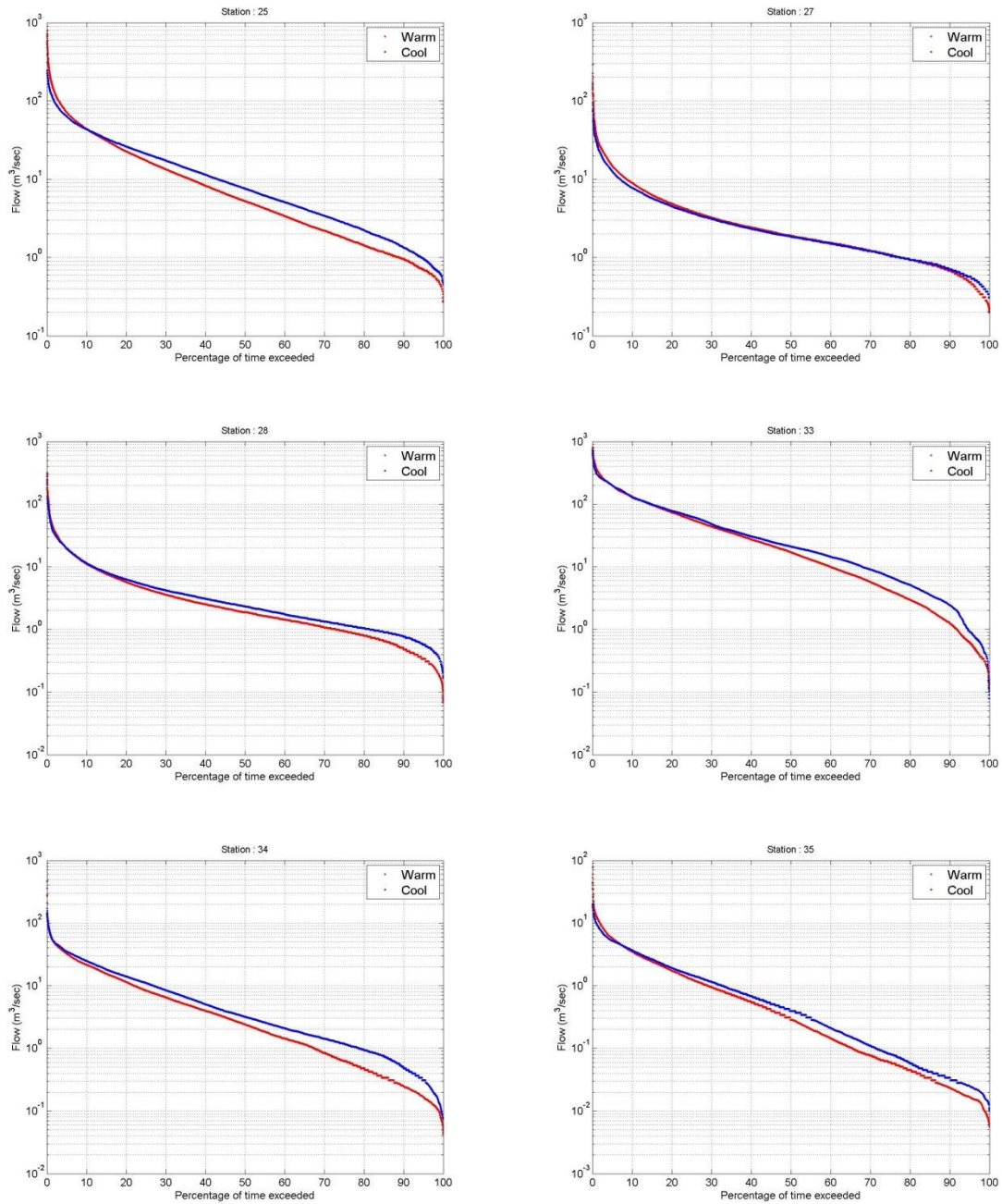


**Figure 44: FDCs of Warm and Cool Phases of AMO (Florida Northern Continental Region)**

Table 28 shows the 7Q10 values for the 6 stations in the northern continental region. The majority (4 out of 6) stations had lower 7Q10 values during the warm phase of

AMO. The remaining 2 stations could not be evaluated because these stations failed the Weibull distribution goodness-of-fit tests.

**Table 28: 7Q10 Values for AMO Warm and Cool Phases (Florida Northern Continental Region)**

<b>Station Number</b>	<b>Warm Phase (m<sup>3</sup>/s)</b>	<b>Cool Phase (m<sup>3</sup>/s)</b>	<b>Lowest 7Q10 Occurrence</b>
25	9.94	15.97	Warm
27	9.63	11.36	Warm
28	3.81	11.04	Warm
33	X	15.10	X
34	X	3.81	X
35	0.23	0.47	Warm

X: Weibull distribution failed goodness-of-fit tests

Finally, Figure 45 shows the cumulative probability streamflow deficit curves. The results in this section were mixed. The greater probability that deficit duration exceeds 30 days occurred in the warm phase of AMO for 2 stations, cool phase of AMO for 2 stations, and the final 2 stations were inconclusive.

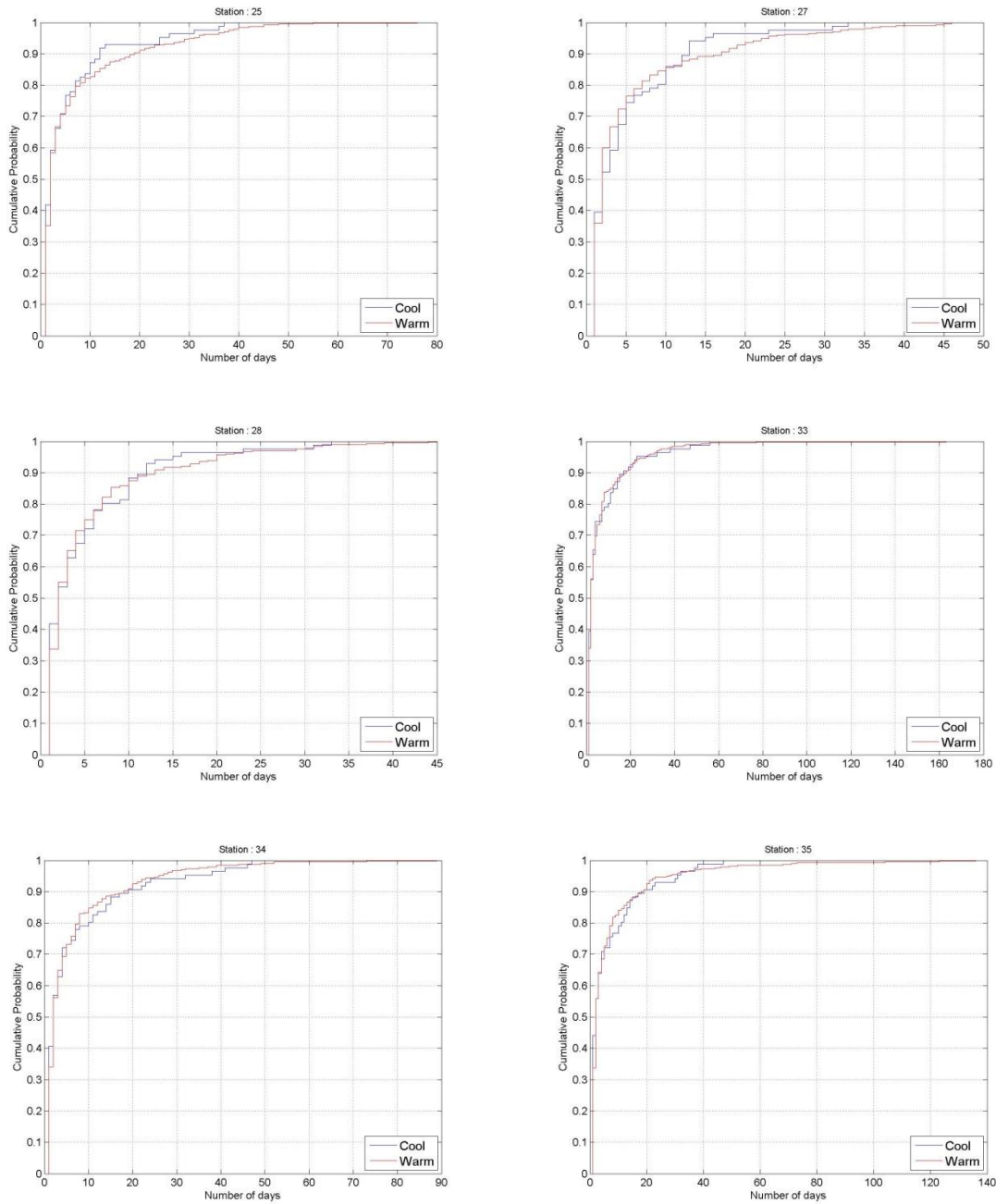


**Figure 45: Cumulative Probability Plots of Streamflow Deficit Duration for Warm and Cool Phases of AMO (Florida Northern Continental Region)**

For the northern continental region of Florida, the anticipated behavior of lower flows during the warm phase of AMO was exhibited in 2 out of 3 indices.

## 6 CONCLUSIONS

Four major atmospheric-oceanic oscillations affect the study area of southeastern United States: ENSO, PDO, AMO, and NAO. These oscillations occur on different timescales and oscillations have varying effects over different geographic locations. This thesis analyzed the influences of these oscillations on streamflow extremes to better understand the spatial and temporal variability of low flows under two different phases on a regional scale.

### 6.1 Contributions of this Study

This study offers an extensive analysis of streamflow extremes in southeastern United States. The spatial and temporal variability of low flows between the warm and cool phases of ENSO, PDO, AMO, and NAO are assessed. First, FDCs were created for the warm and cool phase for each oscillation to quantify which phase has most influence on lower flows. The results of the FDC analysis were then mapped to analyze the spatial variability of this index. Similarly, the 7Q10 value was determined for the warm and cool phase for each oscillation to determine which phase has the lowest 7-day average low flow that occurs on average once every 10 years. Again, these results were also mapped to analyze the spatial variability of this index. A parametric statistical test was applied to the 7Q10 values for each oscillation to determine if statistically significant differences in this low flow index existed between the warm and cool phases. KDEs were then used to analyze the temporal occurrence of the AM7 values for warm and cool phases of each

oscillation. Finally, a streamflow deficit curve was created for the warm and cool phases of each oscillation. Deficit duration values were determined from this curve and subsequently used to create a cumulative probability plot. These plots were used to analyze whether the warm or cool phase of an oscillation was more likely to have deficit durations exceeding 30 days. The results of all of these analyses are discussed for each individual oscillation in the following sections.

### **6.1.1 El Niño – Southern Oscillation**

For the FDC analysis, the first group of stations (1 – 24) had ambiguous results. The second group of stations (25 – 43) had low flows occur predominantly during the La Niña phase. For the 7Q10 analysis, the majority of stations in the whole region had lowest 7Q10 values during La Niña phase years. Results from the two-sample unpaired t-test indicated that the null hypothesis was true for this oscillation, indicating that there was no significant difference between the 7Q10 values for El Niño and La Niña phases of ENSO. For the KDE analysis, the first group of stations had the highest occurrence of AM7 values during the month of September for both the El Niño and La Niña phases. For the second group of stations, there are 2 peak events: first in May/June, then in September. For the first low flow event in May, there are more AM7 occurrences during La Niña phase than El Niño phase. For the second low flow event in September, there are more AM7 occurrences during El Niño phase than La Niña phase. For the deficit duration analysis, the majority of stations in the entire region were more likely to have deficits lasting longer than 30 days during El Niño phase.

### **6.1.2 Pacific Decadal Oscillation**

For the FDC analysis, the majority of stations throughout the whole region had low flows occur during the cool phase of PDO. The same result held true for the 7Q10 analysis: the majority of stations had lowest 7Q10 values during PDO cool phase years. Results from the two-sample unpaired t-test indicated that the null hypothesis was true for this oscillation, indicating that there was no significant difference between the 7Q10 values for warm and cool phases of PDO. For the KDE analysis, the first group of stations (1 – 24) had peak AM7 occurrences in the beginning of September for both phases of PDO. For the second group of stations (25 – 43), there are 2 peak events: first in May, then in September. For the first low flow event in May, there are more AM7 occurrences during cool phase years than warm phase years of PDO. For the second low flow event in September, there are more AM7 occurrences during warm phase years than cool phase years of PDO. For the deficit duration analysis, the majority of stations were more likely to have deficits lasting longer than 30 days during the cool phase of PDO.

### **6.1.3 Atlantic Multidecadal Oscillation**

For the FDC analysis, the majority of stations throughout the whole region had low flows occur during the warm phase of AMO. The same result held true for the 7Q10 analysis: the majority of stations had lowest 7Q10 values during AMO warm phase years. Results from the two-sample unpaired t-test indicated that the null hypothesis was true for this oscillation, indicating that there was no significant difference between the 7Q10 values for warm and cool phases of AMO. For the KDE analysis, the first group of stations (1 – 24) had the most AM7 occurrences for both phases of AMO at the beginning of September. For the second group of stations (25 – 43), there are 2 peak events: first in

May and then in September. For the first low flow event in May, there are more AM7 occurrences during warm phase years of AMO than cool phase years. For the second low flow event in September, there are more AM7 occurrences during cool phase years of AMO than warm phase years. For the deficit duration analysis, the results varied between the 2 station groups. For group 1, the majority of stations were more likely to have deficit durations lasting longer than 30 days occur during the warm phase of AMO. However, for the second group of stations, greater than 30 days of deficit were more likely to occur in the cool phase of AMO.

#### **6.1.4 North Atlantic Oscillation**

For the FDC analysis, the first group of stations (1 – 24) had low flows occurring primarily during the negative phase of NAO. The second group of stations (25 – 43) had more low flows occur during the positive phase of NAO. For the 7Q10 analysis, the results for the first group of stations are ambiguous, but the majority of the stations in the second group had lowest 7Q10 values during the positive phase of NAO. Results from the two-sample unpaired t-test indicated that the null hypothesis was true for this oscillation, indicating that there was no significant difference between the 7Q10 values for positive and negative phases of NAO. For the KDE analysis, the first group of stations has peak AM7 occurrences for both phases of NAO at the start of September. For the second group of stations, both phases of NAO closely follow each other and there are 2 peak occurrences of AM7 values: first during the month of May, and then again during the month of September. For the deficit duration analysis, the majority of stations were more likely to have greater than 30 days of deficit during the positive phase of NAO.

## **6.2 Limitations of this Study**

The first major limitation of this study was that it was restricted to just the South-Atlantic Gulf region of the United States. The area of influence of each of the oscillations studied in this thesis expands beyond this particular region. Further, the influences of oscillations on low flows vary greatly by location. By limiting the scope of this study to just one small region we are unable to understand the full effects of these oscillations.

The second limitation of this study is the relatively small number of streamflow stations used for analysis. While there are thousands of USGS stations in the study region, only 43 met the specific requirements to proceed with analysis. It was critical that only stations included in the HCDN be used for analysis to rule out any anthropogenic input. Additionally, only stations with long-term continuous data were used to ensure the integrity of the analysis.

The third limitation, as a result of the stringent data requirements discussed above, is that some geographic regions of the study area did not have a single representative station. For example, while the whole state of Florida is included in the study domain, there are no stations located in the southern half of the state. This report is thus not indicative of the whole study domain while such large portions of the study area are excluded from analysis.

## **6.3 Recommendations for Future Research**

This research presents an extensive analysis on influences of interannual, interdecadal, quasidecadal, and multidecadal oscillations on regional streamflow extremes. However, there are certain additional analyses that can complement or enhance



this study's work. A major limitation of this study was its limited scope. In this thesis, trends in streamflow extremes and climate variability were studied only in the southeastern United States, specifically HUC region 03. Further analysis is recommended to study the other 20 HUCs in the United States as it is expected that large-scale oscillations may influence hydrology at a large scale (i.e., continental scale).

Another suggestion for future research is the analysis of coupled oscillations on streamflow extremes. In this study, the response of ENSO, PDO, AMO, and NAO on streamflow was studied individually. Further analysis is recommended to study the coupled response of PDO, AMO, and NAO with ENSO to determine if there is any influence of climate variability in regions impacted by ENSO.

Finally, it is suggested that future research be expanded to utilize other common low-flow indices. For example, while this study specifically examined the 7Q10 values of warm and cool phases, another common index is the 4Q3, which is especially important for water quality criteria. Additionally, while this study looked at the deficit durations in the streamflow deficit analysis, future work could evaluate deficit severity (cumulative water deficit) and deficit intensity (the ratio between cumulative water deficit and duration).

## REFERENCES

- Box, G.E.P.; Cox, D.R. An Analysis of Transformations. *Journal of the Royal Statistical Society* **1964**, *26*, 211-252.
- Coley, D.M.; Waylen, P.R. Forecasting Dry Season Streamflow on the Peace River at Arcadia, Florida, USA. *Journal of the American Water Resources Association* **2006**, 851-862.
- Corder, G.W.; Foreman, I.D. *Nonparametric Statistics for Non-Statisticians*; Wiley, 2009.
- Earth Gauge. In-Depth Climate Fact Sheets.  
[http://www.earthgauge.net/climate/climate\\_fact\\_sheets](http://www.earthgauge.net/climate/climate_fact_sheets) (accessed March 29, 2015).
- Goly, A.; Teegavarapu, R.S.V. Individual and Coupled Influences of AMO and ENSO on Regional Precipitation Characteristics and Extremes. *Water Resources Research* **2014**, *50*.
- Gumbel, E.J. *Statistics of Extremes*; Columbia University Press, 1958.
- Hisdal, H.; Streamflow Deficit. *Manual on Low-Flow Estimation and Prediction*; Operational Hydrology Report No. 50; World Meteorological Organization, 2008).

- Hisdal, H.; Gustard, A. The Flow-Duration Curve. *Manual on Low-Flow Estimation and Prediction*; Operational Hydrology Report No. 50; World Meteorological Organization, 2008).
- Hurrell, J.W. Decadal Trends in the North Atlantic Oscillation: Regional Temperatures and Precipitation. *Science* **1995**, *269*, 676-679.
- Hurrell, J.W.; Van Loon, H. Decadal Variations in Climate Associated with the North Atlantic Oscillation. *Climate Change* **1997**, *36*, 301-326.
- Jarque, C.M.; Bera, A.K. A Test for Normality of Observations and Regression Residuals. *International Statistical Review* **1987**, *55*, 163-172.
- Kottek, M.; Grieser, J.; Beck, C.; Rudolf, B.; Rubel, F. World Map of the Köppen-Geiger Climate Classification Updated. *Meteorologische Zeitschrift* **2006**, *15*, 259-263.
- Lilliefors, H.W. On the Kolmogorov-Smirnov Test for Normality with Mean and Variance Unknown. *Journal of the American Statistical Association* **1967**, *62*, 399-402.
- Lins, H.F. *USGS Hydro-Climatic Data Network 2009 (HCDN-2009)*; U.S. Geological Survey Fact Sheet 2012-3047; U.S. Geological Survey, 2012.
- Lins, H.F.; Hirsch, R.M.; Kiang, J. *Water – The Nation’s Fundamental Climate Issue: A White Paper on the U.S. Geological Survey Role and Capabilities*; U.S. Geological Survey Circular 1347; U.S. Geological Survey, 2010.

- Mantua, N.J.; Hare, S.R. The Pacific Decadal Oscillation, *Journal of Oceanography* **2002**, 58, 35-44.
- Nnaji, G.A.; Huang, W.; Gitau, M.W.; Clark, C. Frequency Analysis of Minimum Ecological Flow and Gage Height in Suwannee River, Florida. *Journal of Coastal Research* **2014**, 68, 152-159.
- Pierce, M. Influences of Decadal and Multi-decadal Oscillations on Regional Precipitation Extremes and Characteristics. M.S. Thesis, Florida Atlantic University, , Boca Raton, FL, 2013.
- Rogers, J.C.; Coleman, J.S.M. Interactions Between the Atlantic Multidecadal Oscillation, El Niño/La Niña, and the PNA in Winter Mississippi Valley Stream Flow. *Geophysical Research Letters* **2003**, 30.
- Schmidt, N.; Lipp, E.K.; Rose, J.B.; Luther, M.E. ENSO Influences on Seasonal Rainfall and River Discharge in Florida. *American Meteorological Society* **2001**, 14, 615-628.
- Seaber, P.R.; Kapinos, F.P.; Knapp, G.L. *Hydrologic Unit Maps*; U.S. Geological Survey Water-Supply Paper 2294; U.S. Geological Survey, 1987.
- Searcy, J.K. *Flow-Duration Curves*; U.S. Geological Survey Water-Supply Paper 1542-A; U.S. Geological Survey, 1959.
- Slack, J.R.; Landwehr, J.M. *HCDN: A U.S. Geological Survey Streamflow Data Set for the United States for the Study of Climate Variations, 1874-1988*; U.S. Geological Survey Open-File Report 92-129; U.S. Geological Survey, 1992.

- Smakhtin, V.U. Low Flow Hydrology: A Review. *Journal of Hydrology* **2001**, 240, 147-186.
- Tallaksen, L.; Hewa, G.A. Extreme Value Analysis. *Manual on Low-Flow Estimation and Prediction*; Operational Hydrology Report No. 50; World Meteorological Organization, 2008).
- Teegavarapu, R.S.V.; Goly, A.; Obeysekera, J. Influences of Atlantic Multidecadal Oscillation Phases on Spatial and Temporal Variability of Regional Precipitation Extremes. *Journal of Hydrology* **2013**, 495, 74-93.
- Tootle, G.A.; Piechota, T.C.; Singh, A. Coupled Oceanic-Atmospheric Variability and U.S. Streamflow. *Water Resources Research* **2005**, 41.
- U.S. Geological Survey. Climate Variability and Change. *Facing Tomorrow's Challenges – U.S. Geological Survey Science in the Decade 2007 – 2017*; U.S Geological Survey Fact Sheet 2007 – 3108; U.S. Geological Survey, 2007.
- Wilks, D.S. *Statistical Methods in the Atmospheric Sciences*; Academic Press, 2011.
- World Meteorological Organization. *Manual on Low-Flow Estimation and Prediction*; Operational Hydrology Report No. 50; World Meteorological Organization, 2008).
- Zorn, M.R.; Waylen, P.R. Seasonal Response of Mean Monthly Streamflow to El Niño/Southern Oscillation in North Central Florida. *The Professional Geographer* **1997**, 49, 51-62.